Heterogeneous single-atom catalysis

Aiqin Wang[1]*, *Jun Li*[2]* and *Tao Zhang*[1,3]*

Abstract | Single-atom catalysis has arguably become the most active new frontier in heterogeneous catalysis. Aided by recent advances in practical synthetic methodologies, characterization techniques and computational modelling, we now have a large number of single-atom catalysts (SACs) that exhibit distinctive performances for a wide variety of chemical reactions. This Perspective summarizes recent experimental and computational efforts aimed at understanding the bonding in SACs and how this relates to catalytic performance. The examples described here illustrate the utility of SACs in a broad scope of industrially important reactions and highlight the advantages these catalysts have over those presently used. SACs have well-defined active centres, such that unique opportunities exist for the rational design of new catalysts with high activities, selectivities and stabilities. Indeed, given a certain practical application, we can often design a suitable SAC; thus, the field has developed very rapidly and afforded promising catalyst leads. Moreover, the control we have over certain SAC structures paves the way for designing base metal catalysts with the activities of noble metal catalysts. It appears that we are entering a new era of heterogeneous catalysis in which we have control over well-dispersed single-atom active sites whose properties we can readily tune.

[1]*State Key Laboratory of Catalysis, iChEM (Collaborative Innovation Center of Chemistry for Energy Materials), Dalian Institute of Chemical Physics, Chinese Academy of Sciences, Dalian, China.*

[2]*Department of Chemistry and Key Laboratory of Organic Optoelectronics & Molecular Engineering of Ministry of Education, Tsinghua University, Beijing, China.*

[3]*University of Chinese Academy of Sciences, Beijing, China.*

**e-mail: aqwang@dicp.ac.cn; junli@tsinghua.edu.cn; taozhang@dicp.ac.cn*

https://doi.org/10.1038/s41570-018-0010-1

Over 80% of industrial processes make use of catalysts to increase the rate of a desired reaction. The catalyst is ideally more active for this reaction than it is for side reactions, such that the selectivity is also increased relative to the uncatalyzed process. According to the phases in which a catalyst and the reactant(s) are present, catalysis can be classified as homogeneous, heterogeneous or biological (FIG. 1). Catalysts from all three classes typically have active sites featuring metal centres[1]. Homogeneous catalysts often have metal sites in well-defined coordination environments comprising organic ligands that are either synthetic or proteic in nature. The latter sites are at the centre of enzymes whose activities form the basis of biological catalysts, such as bacteria. Heterogeneous catalysts take the form of either metals or ionic compounds, which can either be bare or serve as substrates for metal clusters or nanoparticles (NPs). Such catalysts are stable even under relatively harsh reaction conditions (such as high temperatures and pressures) and are readily separated from reactants and products. By virtue of this robustness, heterogeneous catalysts dominate large-scale industrial processes.

Heterogeneous catalysis usually occurs at the surface of a solid catalyst, which ideally has a high surface area to volume ratio. For example, smaller metal particles have a higher fraction of surface atoms than do larger metal particles. This fraction not only has an impact on the fraction of metal atoms that are catalytically active (hereafter referred to as metal atom utilization), but also has a substantial effect on selectivity. The metal atom utilization in homogeneous molecular catalysts can reach 100% — a figure that may be orders of magnitude higher than that of heterogeneous catalysts. Indeed, heterogeneous catalysts might feature non-uniform aggregates of hundreds and/or thousands of metal atoms, only a small fraction of which are exposed to reactants. For example, the reactive, coordinatively unsaturated metal atoms at apices, edges, steps and corners usually represent less than 20% of the total metal atoms. Increasing the metal atom utilization of a catalyst is particularly important for heterogeneous catalysts composed of a solid substrate decorated with a platinum group metal (PGM) such as Pd, Pt, Rh, Ir or Ru. Although these metals are the least abundant of the earth's elements, we are dependent on their presence in catalysts to control vehicle emissions, produce chemicals, refine petroleum and serve in fuel cells. Thus, there exists long-standing interest in fabricating heterogeneous metal catalysts that feature atomically dispersed metal atoms as robust active centres (100% atom utilization efficiency). Such an approach would marry the advantages of typical homogeneous and heterogeneous catalysts. Heterogeneous catalysts with atomically dispersed metal atoms have been actively studied in the past several years. Such a catalyst is referred to as a

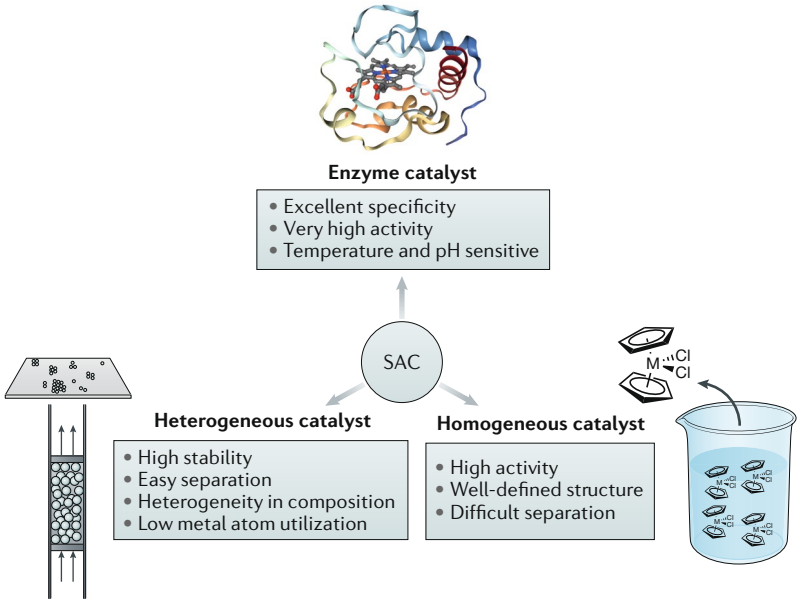

Fig. 1 | **Single-atom catalysts (SACs) incorporate many advantageous features of homogeneous and heterogeneous catalysts.** Enzymes, such as cytochrome *c* peroxidase displayed here[148], can be highly selective and active but are often not robust. Typical homogeneous catalysts have well-defined structures but are not easily recycled because they are difficult to separate from product mixtures. Heterogeneous catalysts can have high stability and are easily separated from reactants and products. However, their active sites may be non-uniform in nature, and only now are technologies emerging that enable their in operando study.

single-atom catalyst (SAC), terminology that was first introduced in a 2011 report from Zhang, Li, Liu and co-workers describing the high CO oxidation activity of single Pt atoms dispersed on FeO_x (REF.[2]).

The development of the now popularized concept of single-atom catalysis coincides with recent advances in both atomic-resolution characterization techniques and theoretical modelling. Used in combination, these methods provide a clear picture of the dispersion of the atoms (or even their exact positions), the bonding between single atoms and the support, and even in operando dynamics of single atoms during catalysis. Already before the emergence of these enabling technologies, many scientists had investigated materials in which (potentially) atomically dispersed metal atoms are on the surface of a support. In 1925, Taylor proposed that the surface of a heterogeneous catalyst has certain catalytically active centres[3]. Furthermore, in the 1960s, scientists drew parallels between the chemisorption of olefins to metal substrates and the well-known Dewar–Chatt–Duncanson model of π-bonding in molecular metal–olefin complexes[4]. Indeed, these early studies showed us that many catalytic reactions depend on isolated atoms rather than ensembles of atoms[5]. At this point, we should emphasize that our definition of SAC does not encompass gaseous metal atoms[6] or monometallic complexes on a surface or in a zeolite[7,8], the latter motif representing a merger of organometallic chemistry and materials chemistry[9,10]. SACs are free of small organic ligands, and the controlled conversion of immobilized metallic complexes to SACs by removal of organic ligands has yet to be realized[11–13].

One of the earliest heterogeneous catalysts with surface metal atoms was reported in 1999 and, featuring atomically dispersed Pt cations on MgO, was found to be as active as metallic Pt NPs are for propane combustion[14]. In the following years, advances in mass spectrometry and soft-landing techniques for decorating surfaces spurred a 'gold rush' in gold nanocatalysis, which drove catalysis research from the nanoscale to the subnanoscale[6,15–17]. Despite these advances, solid materials featuring well-defined catalytically active single metal atoms were very rare[18]. A breakthrough came in 2003 with a report from Flytzani-Stephanopoulos and co-workers[19] describing materials comprising cationic Au or Pt on CeO_2 — heterogeneous catalysts for the water–gas shift reaction (WGS; $CO + H_2O \rightleftharpoons CO_2 + H_2$). Prepared by treatment of CeO_2 with either $H[AuCl_4]$ or $H_2[PtCl_6]$, the materials feature a mixture of highly dispersed Au or Pt atoms and/or clusters along with Au or Pt NPs. The NPs can be removed with CN^- to leave only the cationic Au species, which are apparently strongly bound to surface Ce–O groups. These smaller Au and Pt species are nonmetallic and highly active, in contrast to Au and Pt NPs, which are metallic and catalytically inactive. The active Au and Pt species were found to have cationic character, consistent with their oxophilic nature and small size (on account of electrostatic repulsion). For example, Au^{3+} was thought to substitute for Ce^{4+}, triggering concomitant formation of O^{2-} vacancies to balance charge. However, the interactions between the precious metal cations and the surface were not described in detail, possibly owing to a lack of atomic-resolution technologies. Two years later, Xu and co-workers reported that single Au sites on ZrO_2 are active for the selective hydrogenation of 1,3-butadiene to butenes, although the surface chemistry remained unknown[20]. The material features Au^{3+} sites that are 100% accessible at low loadings. Once more, Au NPs on the support were found to be inactive. In 2007, Lee and co-workers[21] reported that the atomically dispersed Pd species on the surface of mesoporous Al_2O_3 are single-site catalysts for the selective aerobic oxidation of allylic alcohols. The heterogeneous catalyst was prepared from aqueous $[Pd(NH_3)_4](NO_3)_2$, suitably dilute solutions affording atomically dispersed Pd^{2+} species after calcination. In contrast, the use of higher Pd^{2+} concentrations affords only catalytically inactive Pd NPs. Strong evidence for the structure of the two systems came from extended X-ray absorption fine structure (EXAFS), which gave bond lengths consistent with Pd–O and Pd–Pd groups, respectively. However, while it was clear that dilute precursor solutions can afford materials in which Pd^{2+} is present and bound to four oxo ligands, the location of the cations and their interactions with the support remained elusive. As mentioned above, Zhang, Li, Liu and co-workers[2] reported in 2011 that single Pt atoms dispersed on FeO_x are highly stable (for example, towards sintering) and active for CO oxidation. Arguably the most important aspect of this work was the combined use of high-angle annular dark-field scanning transmission electron microscopy (HAADF-STEM), spectroscopy and computational techniques to elucidate both the bonding between the single Pt atoms

and the FeO_x support and the catalytic mechanism. The team suggested the term SAC, which is defined as a supported metal catalyst exclusively containing isolated monometallic active sites on a surface. Such materials in which single metal atoms M are dispersed on a support have been denoted M_1/support (for example, Pt_1/FeO_x) to make it clear that the material is both atomically dispersed and heterogeneous[2,22].

At this point, it is useful to define a single-site heterogeneous catalyst (SSHC) as a system in which many identical catalytically active sites are dispersed on a solid surface. Introduced in 2005 by Thomas, these materials only have a single type of active site, which need not be mononuclear[23]. In general, SACs are not a subclass of SSHCs because SAC active sites are not necessarily uniform owing to the non-uniform nature of most solid supports, especially in practical industrial catalysts. Indeed, although we know that single metal atoms may serve as catalytically active sites in many reactions, the unambiguous determination of the one or more active site geometries of SACs, as is the case for most heterogeneous catalysts, remains a challenge. We stress again that our definition of SACs does not extend to gaseous single atoms — to a great extent, the so-called single atom cannot complete the whole catalytic cycle alone. For example, the activity of a single metal atom M typically relies on interactions with a number of heteroatomic ligands (such as oxos) that anchor it to metal atoms of the substrate. Here, the electronic structure and reactivity of M are very sensitive to the number of oxos that bind M. One way to probe electron density at any metal site M is to expose the heterogeneous catalyst to CO and study the ν_{CO} bands using infrared spectroscopy. In general, SACs treated with CO give rise to broad ν_{CO} bands composed of overlapping stretching modes from non-equivalent active sites[2]. A true SSHC would give rise to a sharper band because "the single site may consist of one or more atoms, but each site is structurally well-characterized, spatially isolated, and has the same energy of interaction between it and a reactant as every other single site, just as the single sites in homogeneous molecular catalysts are" (REF.[23]). According to this definition, a certain subset of SACs — those with more than one type of active site — are not SSHCs. Conversely, SSHCs with multinuclear active sites are not SACs.

The difficulty associated with obtaining a perfectly uniform solid material means that the active sites of most SSHCs reported to date are not single atoms but rather take the form of well-defined molecular catalysts grafted onto oxide or zeolite surfaces. Most likely, at extremely low catalyst coverage, one has a SAC with uniform active sites — a true SSHC. We consider the terms catalytic active site and SSHC rather broad and structurally vague. In contrast, it is well understood what a SAC is, and recent advances in electron microscopy techniques enabling us to directly visualize single atoms have led to the blossoming of this field. Thanks to the mononuclear nature of the active sites, SACs not only have maximal atom utilization efficiency but also offer opportunities for tuning reaction rates and selectivities, thus bridging the gap between homogeneous and heterogeneous catalysts. Therefore, SACs may provide a good platform for understanding structure–activity relationships on an atomic scale.

It is possible that single surface metal atoms have roles in many previously known reactions catalysed by known materials. Confirmation of this reactivity has only recently become possible through rapid developments in both atomic-resolution characterization technologies and advanced theoretical modelling and simulations. Using these tools allows one to determine whether or not a system is a SAC. In particular, by using aberration-corrected high-angle annular dark-field scanning transmission electron microscopy (AC-HAADF-STEM) we can clearly identify single metal atoms on supports, provided the metal atom of interest has a much higher atomic number than the support elements[24]. X-ray absorption spectroscopy (XAS) is also useful, and under either ex situ or in situ conditions, X-ray absorption near-edge structure (XANES) can provide information about metal oxidation states. The complementary technique extended X-ray absorption fine structure (EXAFS) gives information regarding the local coordination environment of central metal atoms as a weighted average[25]. Other powerful techniques useful for identifying the exact structure of SACs include Fourier-transform infrared (FTIR) spectroscopy and scanning tunnelling microscopy (STM)[26,27]. The materials can also be studied computationally using either density functional theory (DFT) or higher levels of theory to afford reliable models of active sites. Moreover, one can simulate catalytic cycles and get energy barriers for each elementary step. It is interesting to note that now, with access to modern characterization methods, we have revisited 'old' reactions that were long believed to be catalysed by nanoclusters or nanoparticles. In some cases, it was found that single metal atoms rather than clusters are the active species. For example, in 1985, Hutchings[28] correlated the catalytic activity of carbon-supported metal chlorides for acetylene hydrochlorination with the standard reduction potential of the metal cations. It was reasoned that Au^{3+} cations were more active than Hg^{2+} on account of the lower reduction potential of the latter. The clear correlation in this pioneering work is very much consistent with the materials behaving as SACs. At the time, the unavoidable formation of Au NPs precluded clear identification of the true active site in the $AuCl_3$-derived system. Only in 2017, by making use of in situ EXAFS under catalytic working conditions, was it found that $AuCl_3$ converts into AuCl units that are the true active sites in this carbon-supported catalyst[29].

SACs can exhibit distinct and often outstanding performance in many industrially important reactions, including thermochemical, electrochemical and photochemical conversions. The SAC motif not only enables 100% atom utilization but has unique geometric and electronic properties stemming from the absence of metal–metal bonds and the cationic (or sometimes anionic) nature of the isolated catalytic sites. The unique reactivity of SACs is exemplified in the chemoselective hydrogenation of substituted nitroarenes containing multiple reducible functional groups. Indeed, the Pt_1/FeO_x SAC preferentially binds nitro groups and thus mediates formation of the corresponding substituted anilines

with exceptionally high selectivity[30]. When the single metal atoms sit atop a metal support, we speak of a type of SAC known as a single-atom alloy (SAA). One example of an SAA is a material in which Zn atoms are dispersed on bulk Pd, a system that is active for the semi-hydrogenation of acetylene to ethylene. This SAA features Pd–Zn–Pd active sites that semi-hydrogenate acetylene even at relatively high conversions; ethylene apparently does not outcompete with acetylene for catalytic sites[31]. In terms of CO_2 hydrogenation, single Rh atoms supported on TiO_2 are highly selective catalytic sites for the reverse WGS reaction ($CO_2 + H_2 \rightleftharpoons CO + H_2O$), and Rh NPs are superior in the methanation reaction ($CO_2 + H_2 \rightleftharpoons CH_4 + H_2O$). We can account for these reactivities by considering the charge on the Rh sites: single SACs feature Rh centres with greater positive charge such that π-backbonding to CO is weak, allowing for rapid turnover of the catalyst in the reverse WGS reaction[32]. When supported on TiN, single Pt or Pd atoms, in contrast to many oxygen reduction reaction (ORR) catalysts, are selective for the $2\,H^+/2e^-$ reduction of O_2 to H_2O_2 in preference to the $4\,H^+/4e^-$ reduction that affords two molecules of H_2O (REF.[33]).

Some SACs exhibit superior stability relative to their nanoparticle counterparts. As we noted above, strong covalent bonding between single metal sites and the support was cited as the reason why supported Au NPs can be removed with CN^-, while the isolated Au^{3+} ions remain in the CeO_2 support. Moreover, these single Au (or Pt) sites on CeO_2 are highly resistant to thermal sintering during CO oxidation catalysis[34,35]. Similarly, single Pt atoms supported on mesoporous Al_2O_3 remain isolated and active even after the catalytic hydro-reforming of *n*-hexane to branched isomers is carried out at 550 °C for 48 h (REF.[36]).

Recent work has greatly expanded the chemical space occupied by known SACs. The first examples discovered were oxide-supported noble metal SACs, which were followed by SAAs[37] and then single transition metal atoms bonded to N-doped carbon supports[38] — the latest additions to the family. The original wet-chemical approaches to preparing SACs have been complemented by new methods that can afford materials with high densities of surface single atoms and more tuneable metal–support interactions. Initially developed for applications in materials science, these synthetic methods include photochemical reduction[39], iced photochemical reduction[40], atomic-layer deposition (ALD)[41] and the pyrolysis of metal–organic frameworks (MOFs)[42]. Synthesis aside, considerable efforts have also been devoted to addressing important issues regarding SACs, such as how single atoms are stabilized on supports, the catalytic roles of the single atoms and the surrounding support atoms and the dynamics and stability of active sites during catalysis. The rapid growth in SAC research has seen the topic covered in some recent reviews[22,43–47], although there are still holes in our knowledge. Obtaining a more complete picture of single-atom catalysis will require further experimental and theoretical efforts, particularly those targeted at understanding the structure–activity relationships of SACs, which will enable the rational, bottom-up, atom-by-atom design of supported metal catalysts. In this Review, we provide an overview of single-atom catalysis that includes summaries and critical evaluations of recent advances in this thriving area. We place particular emphasis on the key scientific questions surrounding SACs: how are single atoms stabilized on various supports, and what unique features are responsible for the distinct performances of SACs relative to conventional NP catalysts?

Anchoring single atoms on supports

The surface free energy of a metal greatly increases when it is divided into smaller particles[22], such that single atoms are often susceptible to aggregation during pre-activation and reaction processes. Overcoming this propensity for single metal atoms to aggregate necessitates the formation of strong bonds between the atoms and the underlying support — a central goal in the study of SACs. Such interactions affect not only the stability of single atoms but also the nature of the binding sites and the reactions for which a SAC is competent.

SACs on oxide supports. Oxides are the most widely used supports for metal catalysts. Having high specific surface areas, abundant metal or oxygen vacancies and surface OH groups, oxides have many advantages over other supports in stabilizing single metal atoms. Of particular use are oxides of reducible metal ions such as Ce^{4+}, Ti^{4+} and Fe^{3+}, among others. We now describe some SAC systems, choosing a range of materials that exemplify the properties of the many supports available to us.

Fe oxides are typical 3*d*-metal-based supports used to stabilize single precious metal atoms. Fe is redox active, such that the oxide assumes different phases depending on the reaction and/or pretreatment methods used. For example, haematite (α-Fe_2O_3) and maghemite (γ-Fe_2O_3) predominate under oxidizing conditions, while magnetite (Fe_3O_4) and wüstite (FeO) are present under reducing conditions. The uncertainty regarding the composition of Fe oxides makes identifying the precise location of precious metal atoms on Fe oxide supports challenging. Adding to these complications, surface OH groups may also stabilize or destabilize the nearby single atoms through second coordination sphere effects. Following our paper describing single Pt atoms stabilized by ionic and covalent bonding to FeO_x (REF.[2]) (FIG. 2), reports also emerged of other precious metals — including Ir and Au — forming stable SACs dispersed on Fe_2O_3 (REFS[48–50]). These new materials exhibit distinct activities for topical reactions such as CO oxidation[48], the WGS reaction[49] and NO reduction[50]. EXAFS data for the Pt_1/FeO_x material point to the Pt coordination number being approximately three, such that each of the active sites features three Pt–O bonds. This active site model is plausible according to DFT calculations, which suggest that the arrangement is most stable when the Pt atoms are at the O3-terminated surface of Fe_2O_3(001). Below these Pt atoms lies a third layer composed of Fe atoms (FIG. 2a). This is a situation in which one of the Fe atoms on the O3-terminated surface is replaced by a Pt atom, a model consistent with AC-HAADF-STEM images. The greater size of Pt relative to Fe means that the Pt atom cannot fit

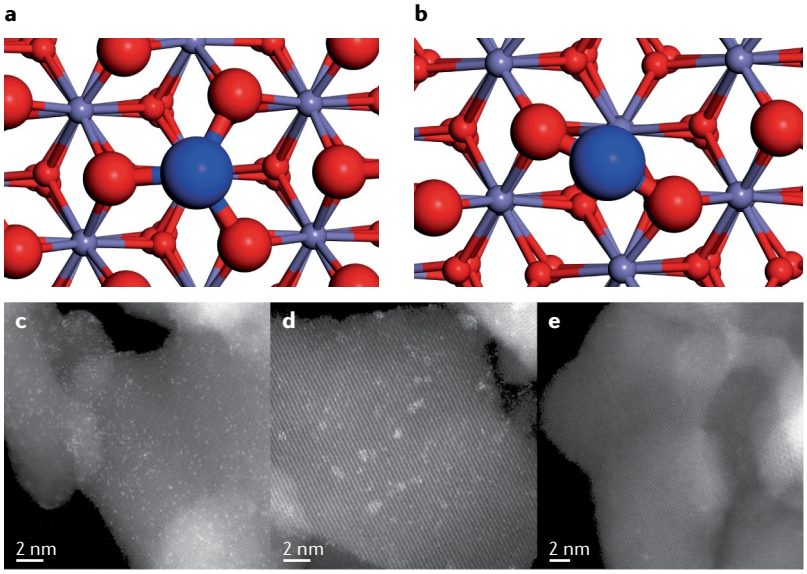

Fig. 2 | **Atomic structures of Pt_1/FeO_x catalysts. a** | Density functional theory calculations suggest a structure for Pt_1/Fe_2O_3 in which Pt binds three O atoms and lies above an Fe vacancy on the O3-terminated surface of Fe_2O_3(001). **b** | The calculated structure of Pt_1/Fe_3O_4 is similar except that Pt is bound to only two O atoms. **c**–**e** | High-angle annular dark-field scanning transmission electron micrographs of the Pt_1/FeO_x surface allow visualization of the active sites. **c** | A 2.5 wt% Pt/Fe_2O_3 sample after calcination, as modelled in part **a**. The bright spots are single Pt centres. **d** | The micrograph shows a calcined 2.5 wt% Pt/Fe_2O_3 sample after exposure to reducing conditions. Reduction triggers the aggregation of Pt atoms, with the resulting clusters being visible as bright regions. **e** | Instead, if a more dilute calcined sample is reduced, one can maintain the isolation of Pt centres, as is the case with 0.08 wt% Pt/Fe_3O_4. The micrograph here depicts a low coverage of atomically dispersed Pt, as modelled in part **b**. This figure contains unpublished observations (T.Z.) related to the Pt_1/FeO_x system[2].

in the plane with the other Fe atoms but instead is above the plane of O atoms such that it is very much accessible to organic reactants. This model appears reasonable and can account for the high thermal and oxidative stability of the Pt_1/Fe_2O_3 catalyst during calcination in air at high temperatures (FIG. 2c). When the catalyst is present in reactions involving reducing atmospheres such as H_2, the support surface and even the bulk support itself undergo reduction to Fe_3O_4, which interacts differently with the single Pt atoms[2,22,51] (FIG. 2b). In this Pt_1/Fe_3O_4 material, each Pt atom bonds to only two O atoms, in agreement with EXAFS data collected for freshly reduced Pt_1/FeO_x. If the surface coverage of Pt is sufficiently high, the aggregation of Pt atoms accompanies the reduction of Fe_2O_3 to Fe_3O_4 (FIG. 2d). Thus, maintaining the isolation of Pt atoms in reducing environments necessitates keeping the density of Pt atoms very low, which is achievable by using Pt loadings below 0.1 wt% (FIG. 2e).

Consistent with our admittedly simplified structural model of the Pt_1/Fe_3O_4 SAC are later results of a systematic study of single adatoms on Fe_3O_4(001). STM and X-ray photoelectron spectroscopy, in combination with DFT calculations[52–56], show that the Fe_3O_4(001) surface, which undergoes a $(\sqrt{2}\times\sqrt{2})R45°$ reconstruction triggered by the subsurface Fe vacancy, features a pocket in which a single metal atom can be accommodated. The single metal atoms are coordinated to two O atoms at positions without second-layer interstitial Fe atoms. The high stability of the metals in the binding pocket is proposed to originate from the charge and orbital ordering within the first subsurface layer. Apart from Pt, other noble metals such as Au, Pt and Pd, as well as 'less noble' metals such as Ni and Ag, can be stabilized in such a configuration, provided they are present at low surface coverages. In contrast, Ti, Zr, Co and Mn each prefer to occupy the subsurface cation vacancy sites to form ferrite-like compounds[54,55]. A single metal atom can also be located at an O vacancy, in which case it can bond to metals in the support[57,58].

CeO_2 is an important 4*f* oxide that can undergo reduction and stabilize single metal atoms, either by substitution at a Ce site or by bonding to surface O or OH groups without ejection of a Ce cation. Such noble metal/CeO_2 SACs are expected to be stable and useful for a variety of industrially important reactions, including CO oxidation, the WGS reaction and CH_3OH stream reforming (MSR). The stability of single metal atoms on CeO_2 is dependent on the morphology and dimensions of the surface. Although single Au or Pt atoms can be dispersed on CeO_2 at low metal loadings (<0.5 wt%) using wet-chemistry methods[34,35], the bonding between Au or Pt and CeO_2 is not fully understood. Towards this, DFT calculations, in combination with XAS, can provide plausible structural models. For example, bulk CeO_2 can be modelled as a cuboctahedral $Ce_{40}O_{80}$ nanoparticle to study the origins of single Pt atom stabilization on different facets of 'nano CeO_2' (REF.[59]). The calculations show that Pt preferentially adsorbs on the polar {100} facets by donating $1e^-$ to each of the two nearby Ce^{4+} cations ($Pt \rightarrow Pt^{2+}$, $2Ce^{4+} \rightarrow 2Ce^{3+}$), forming a PtO_4 core that assumes a square-planar structure — a geometry in which Pt^{2+} ($5d^8$) is stabilized. This electron transfer makes the oxo ligands more basic, such that the adsorption energy is 678 kJ mol^{-1} — a value much higher than the cohesive energy of bulk Pt (564 kJ mol^{-1}). This implies that isolated Pt^{2+} sites dispersed on {100} facets of nano CeO_2 are thermodynamically stable with respect to sintering. Further calculations show that such an O_4 metal-binding site can also host a single Pd or Ni atom[60]. The polar CeO_2(100) surface is less stable than the CeO_2(111) surface, a fact that may contribute to the strong binding of metals at the former. Nevertheless, a model study on single-crystalline CeO_2(111) demonstrated that single Pt^{2+} ions are stabilized at monoatomic step-edge sites of CeO_2(111) in the form of planar PtO_4 moieties[61]. In contrast to the DFT study using nano CeO_2, in this single-crystal study the formation of Pt^{2+} is not accompanied by the reduction of Ce^{4+}; instead, the oxidation of Pt^0 to Pt^{2+} is due to the formation of ionic Pt–O bonds through reaction with adventitious O_2 under ultrahigh vacuum. Monoatomic step edges are ubiquitous defects in oxides, and the number of these edges can be changed by varying the morphology and particle size[62]. In place of nano or single-crystal CeO_2, one can use powdered CeO_2 as a substrate for practically accessible SACs. Indeed, Au_1/CeO_2 SACs can be prepared using wet chemistry at low Au loadings (0.05 wt%), with the HAADF-STEM images of the product suggesting that the Au sites occupy Ce vacancies, in contrast to the above Pt systems[34]. Another synthetic method involves atom trapping, an approach

that enables the preparation of SACs featuring isolated Pt sites on CeO_2 (REF.[35]). Moreover, CeO_2 in the form of polyhedral or nanorod morphologies is more effective than CeO_2 nanocubes in anchoring single Pt atoms. HAADF-STEM images indicate that single Pt cations can replace step-edge Ce atoms. A similar square-planar PtO_4 motif was also proposed to exist in Pt_1/PMA (PMA = phosphomolybdic acid), in which single Pt atoms bind four bridging oxos in fourfold symmetric hollow sites on the PMA surface[63]. In the case of the Pd/zeolite SAC Pd_1/ZSM-5 (ZSM-5 = $Na_4Al_4Si_{92}O_{192}$), each Pd centre bonds to four O atoms on the internal surface of the micropores. These PdO_4 sites are active for the low-temperature oxidation of CH_4 to CH_3OH (REF.[64]). The excellent stability of square-planar MO_4 fragments for noble metals parallels the preferred coordination of noble metal d^8 ions in mononuclear complexes[65]. Although the MO_4 motif is stable towards further oxidation, it is less stable under a reducing atmosphere. For example, exposure of M_1/CeO_2 to H_2 at high temperatures can result in the M^{2+} sites undergoing reduction to M^0, after which, under certain conditions, sintering may occur owing to the formation of M–M bonds.

Al_2O_3 is one of the most widely used metal oxide supports for precious metals in industrial catalysis. This *p*-block oxide has desirable textural properties and binds noble metals strongly enough to afford SACs with excellent mechanical and thermal stability. Nevertheless, Al^{3+} is redox inactive under most conditions, such that Al_2O_3-supported SACs are less explored in comparison with the aforementioned reducible metal oxides. The low reduction potential of Al^{3+} limits charge transfer between prospective single metal sites and Al_2O_3, a driving force for the single metal centres to undergo oxidation and bind oxos instead of remaining in a low valent state and undergoing sintering. However, one advantage that Al_2O_3 has over reducible oxides is its superior thermal stability, which, as evidenced by recent results, may open alternative synthetic paths to thermally stable SACs[36,66].

The thermal stability of Al_2O_3 — including the industrially relevant γ-Al_2O_3 form — allows one to operate at high temperatures. Indeed, atomically dispersed Pd on La^{3+}-doped Al_2O_3 can be prepared by impregnating the support with $[Pd(NH_3)_4](NO_3)_2$ solution and calcining in air at 700 °C (REF.[66]). AC-HAADF-STEM and XAS data show that by using a relatively low Pd loading of 0.5 wt%, one can ensure that all Pd is present exclusively as single Pd^{2+} ions that are stabilized by nearby La^{3+} ions. Exposure of the material to CO triggers reduction of the Pd^{2+} sites to Pd^{1+}, which are highly active centres for CO oxidation (approximately an order of magnitude more active than metallic Pd). Based on DFT calculations, a structural model was proposed in which Al^{3+} in a fourfold hollow site is replaced by La^{3+}. In what would be the location of an adjacent Al^{3+} ion now resides a Pd^{2+} site as part of a stable square-planar PdO_4 motif, two oxos of which are shared with La^{3+}. As of yet, it is unclear how and why La^{3+} doping apparently stabilizes the nearby single Pd^{1+} sites during catalysis.

Mesoporous Al_2O_3 has also proved to be a useful support and has been used in a convenient one-pot sol–gel method in which suitably dilute precursor solutions can afford atomically dispersed single metal sites. For example, at low Pt loadings of 0.2 wt%, one obtains a material with single Pt sites[36], with Pt being cationic and existing in the now familiar square-planar PtO_4 fragments according to AC-HAADF-STEM and XAS data. When on Al_2O_3, these PtO_4 fragments are exceptionally stable under harsh oxidation and hydrogenation reactions, such as 60 heating cycles at 100–400 °C conducted during CO oxidation over 1 month or *n*-hexane hydro-reforming at 550 °C for 48 h. It should be noted that the PtO_4 motif may be only one of several plausible structural models. Earlier results obtained using ultrahigh-field solid-state magic-angle spinning NMR spectroscopy suggest that Pt cations do not substitute at Al^{3+} sites but rather are bridged to pentacoordinate Al^{3+} through shared oxo ligands[67].

The examples of oxide-supported SACs described above illustrate that single atoms and/or ions can be stabilized through bonding to oxo ligands to afford MO_n (n = 2–4) motifs with coordination geometries resembling mononuclear homogeneous catalysts. A common feature is that the M sites in MO_n motifs are all cationic because they form by low-valent M reducing the neighbouring cations of the support. Usually, the cationic nature of the single metal centres makes them at least somewhat oxophilic, and the metal sites, on account of electrostatic repulsion, are stable towards sintering under an oxidizing atmosphere. Under a reducing atmosphere, however, the MO_n motif may not be as stable, and, especially at high temperatures, M cations may be reduced to M^0. These neutral atoms are less oxophilic and interact less strongly with the support, such that the cohesive energy of NPs may not be overcome to avert sintering. Therefore, one needs to carefully choose conditions for reduction reactions and find an optimal support composition and morphology such that a metastable or globally stable SAC can be viable.

SACs on supports with other heteroatoms. The stabilizing effect of bonding between single transition metal atoms and/or ions and the support is not limited to materials containing oxo ligands. Other donor atoms can also be effective, particularly when carbon-rich supports are concerned. For example, N atoms in carbon-rich supports not only strongly anchor individual metal centres but also modify the electronic properties of the carbon. Relative to metals deposited on undoped supports, metal sites on N-doped carbon materials can exhibit higher activity and/or selectivity in a variety of electrocatalytic processes. Example of such SACs include materials in which single PGM atoms are dispersed on N-doped carbon nanofibres. DFT calculations for these materials suggest that each PGM atom is likely coordinated to two pyridinic N atoms at the edge of the graphitic sheets (FIG. 3a), with the bond strength being dependent on the electronic properties of the metal according to the order Ru > Pt > Pd (REF.[68]). When present in such a coordination sphere, the single metal centres are positively charged (for example, Pt and Pd exist in the +II oxidation state) and resemble classic Werner complexes of 2,2′-bipyridine or 1,10-phenanthroline (phen).

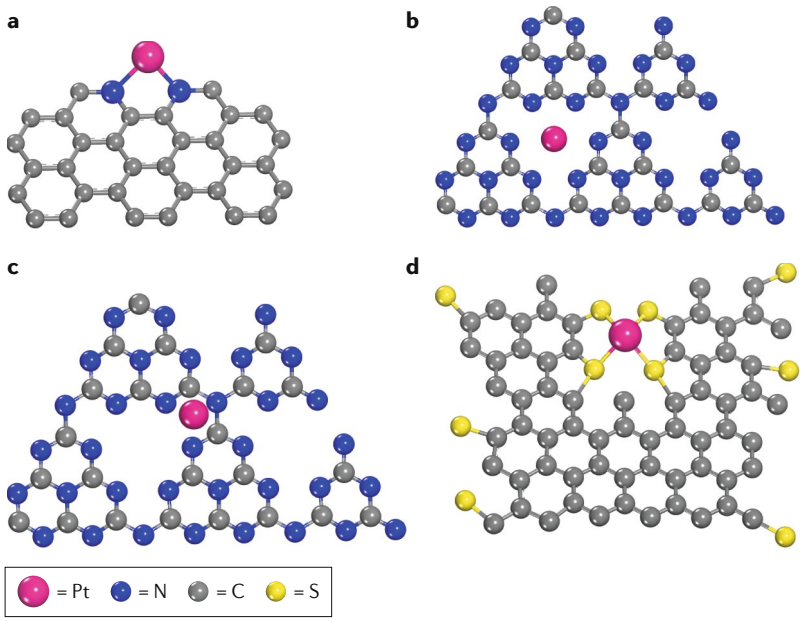

Fig. 3 | **Single Pt centres can bond to N-rich or S-rich regions in doped carbonaceous supports. a** | The edges of N-doped graphene sheets can feature pairs of pyridinic N atoms that bind Pt much as 2,2′-bipyridine does[68]. **b** | Pt atoms are also well hosted in cavities of mesoporous polymeric graphitic C_3N_4 that contain six N atoms[69–72]. **c** | Alternatively, Pt atoms can lie above the C_3N_4 plane and bind three N atoms and two C atoms in a half-sandwich structure[70]. **d** | In S-doped carbons, divalent Pt can bond to thiolate and thioether S centres in a distorted square-planar geometry[73].

In addition to N-doped carbon materials, more well-defined solids, such as mesoporous polymeric graphitic carbon nitride (mpg-C_3N_4), are also useful supports to which single PGM atoms can be anchored. The pores of mpg-C_3N_4 are ideally suited to binding metals, as each has six N atoms derived from the unique tri-*s*-triazine motif. Using Pd or Pt loadings of up to 0.5 wt%, one can obtain 100% atomic dispersion of metal centres across mpg-C_3N_4 (REFS[69,70]). DFT calculations and EXAFS data fitting allow one to obtain detailed structural models and probe the interaction of the PGM atoms with the mpg-C_3N_4 support. The N-rich cavities are the most favourable sites to host PGM centres (FIG. 3b), as indicated by the large magnitudes of the calculated metal binding energies (−2.17 eV and −2.95 eV for Pd and Pt, respectively)[71]. Moreover, based on the theoretical analysis of the charges, there are strong electronic interactions between the single metal centres and the neighbouring pyridinic N atoms of mpg-C_3N_4. The charges of the Pd and Pt centres on mpg-C_3N_4 (+0.40 and +0.27, respectively) are lower than those of Pd and Pt centres on Fe_2O_3 (+0.61 and +0.45, respectively), reflecting the hardness of the oxo ligands and the propensity of Fe_2O_3 to undergo reduction[72]. Despite the favourable interactions that the sixfold cavity can have with PGM centres, the experimental results are not always consistent with the DFT-predicted results. For example, EXAFS data support an alternative structure in which single Pt atoms are located above the mpg-C_3N_4 plane and bind three N atoms and two C atoms[70] (FIG. 3c).

Aside from carbon materials containing N atoms, S-containing materials can also host atomically dispersed metal centres and have been converted into SACs. Particularly with regard to soft metal centres, soft Lewis bases, such as S donors, can bind more strongly than N donors. Indeed, S-doped zeolite-templated carbon prepared by chemical vapour deposition (CVD) is an excellent support for single Pt atoms[73]. The relatively high level of doping (up to 17 wt% S) affords many binding sites, such that up to 5 wt% Pt can be dispersed as single metal centres. EXAFS data support a model (FIG. 3d) wherein each Pt centre is in the +II oxidation state and is bonded to four S atoms at graphene edge sites. Such a structure is analogous to homogeneous organometallic Pt complexes[74], suggesting that the SACs indeed can be viewed as a conceptual bridge between homogeneous and heterogeneous catalysts[22].

Ternary M–N–C materials (where, for example, M = Co, Fe, Ni or Cu) feature atomically dispersed M centres bonded to neighbouring N atoms[38]. M–N–C materials have been intensely investigated as promising candidates to replace Pt in a variety of electrocatalytic reactions. Despite this research attention, it is only very recently, sparked by the rapid development of SACs, that we have been able to prepare atomically dispersed M–N–C (M–N–C SAC) materials[38,75–84]. Such products can be prepared either by synthesizing N-doped carbons and introducing M in a subsequent step or by a single step involving the pyrolysis of metal complexes bearing ligands containing both N and C, such as phthalocyanine, porphyrin and phen. To avoid the sintering of single M atoms into nanoparticles during pyrolysis, it is important that the molecular precursor is present at low concentrations and is rich in N, such that suitable M chelation sites are plentiful[38,84].

A recently developed approach to M–N–C SACs makes use of zinc imidazolate frameworks as precursors[42,79]. A fraction of the Zn^{2+} sites can be substituted for Co^{2+}, and pyrolysis of the framework at temperatures above 800 °C causes the organic ligands to reduce the metal. The thus-formed Zn evaporates to leave Co–N–C, a material with isolated Co sites strongly bonded to N atoms in a framework (the material featuring Co atoms bonded to *x*N atoms is denoted M–N_x). Related work involves pyrolysis of the zinc imidazolate framework hosting [Fe(2,4-pentanedionato)$_3$] molecules inside its pores, a procedure that affords an Fe–N–C material. Both of these pyrolysis methods afford products with a high loading of single atoms: up to 4 wt% for Co–N–C and 2 wt% for Fe–N–C.

Neither the synthesis of M–N–C SACs nor the structural identification of their M–N_x sites is a trivial task[38,81–84]. It is not yet clear if M–N–C SACs typically feature an overwhelmingly favourable common ligand pocket for the catalytically active M sites. Otherwise, it could be possible that a great diversity of these ligand pockets exist, with a different type forming depending on the reaction precursors and conditions. Characterization efforts have recently allowed structural identification of M–N_x sites in Co–N–C (REF.[38]) and Fe–N–C (REF.[84]) materials prepared by the pyrolysis of [Co(phen)$_2$(OAc)$_2$]/Mg(OH)$_2$ and Fe(OAc)$_2$/phen/MgO mixtures, respectively, followed by acid treatment. Although both syntheses make use of phen and the

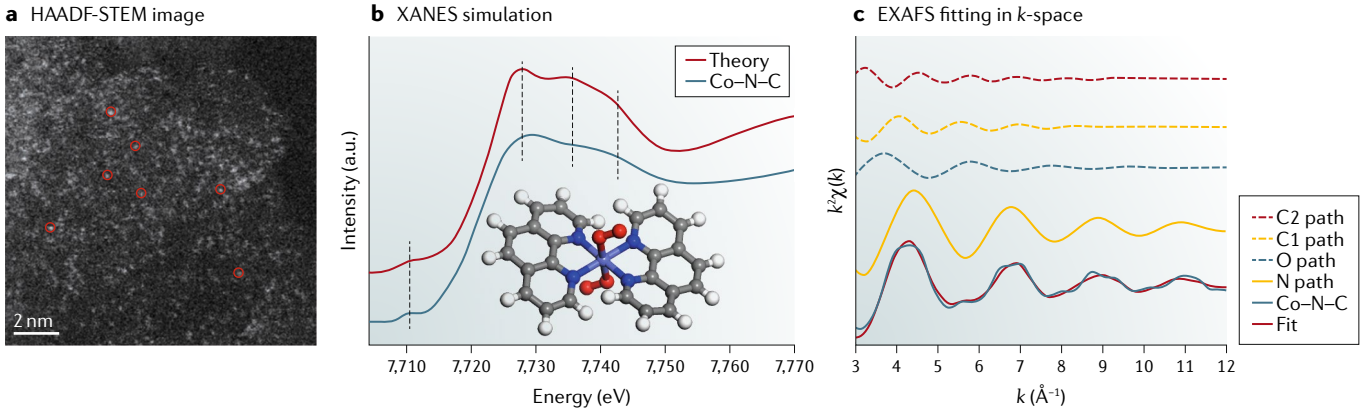

Fig. 4 | **Structural identification of a Co–N–C single-atom catalyst. a** | High-angle annular dark-field scanning transmission electron microscopy (HAADF-STEM) image of the catalyst reveals the locations of atomically dispersed Co cations (selected sites circled). **b** | Information regarding the oxidation state of Co comes from X-ray absorption near-edge spectroscopy (XANES), with experimental (blue) and theoretical (red) spectra agreeing well. The theoretical spectrum was simulated using a $[Co(phen)_2(O_2)_2]$ model complex. **c** | In turn, data regarding the coordination environment around Co come from extended X-ray absorption fine structure (EXAFS) measurements. Fitting the spectra in *k*-space allows one to isolate the contributions of Co–N (yellow line), Co–O (dotted blue line), Co–C1 (dotted yellow line) and Co–C2 (dotted red line) atomic pairs, consistent with the $[Co(phen)_2(O_2)_2]$ model. The sum of these contributions affords a fit (red traces) that agrees well with the experimental data (blue trace). Adapted from REF.[38], CC-BY-3.0.

same pyrolysis procedure, the resulting Co–N–C and Fe–N–C SACs have very different $M–N_x$ structures. In the Co–N–C SAC[38], isolated Co^{2+} ions are coordinated to four N atoms in non-planar CoN_4 units, the two apical sites of which are each occupied by an O_2 ligand (FIG. 4). In contrast, Mössbauer spectroscopy indicates that the Fe–N–C SAC features $Fe–N_x$ sites with different numbers of N donor atoms ($x = 4$, 5 and 6) and different Fe oxidation states (+II and +III)[84]. Evidently, the identity of the metal ions templating the M–N–C SAC affects the structure of the resulting N-donor pocket. Despite the utility of XAS and DFT, the structures of M–N–C SACs can be unclear because XAS data can often be fit to multiple plausible models, in part owing to the inability of the technique to distinguish C atoms from N atoms. Thus, it becomes necessary to make use of complementary techniques to identify the structure of $M–N_x$ active sites in M–N–C SACs.

The addition of alkali metal cations to SACs alters the electronic structures of the catalysts and can promote reactivity. Although the electronic consequences of the presence of alkali metal cations are understood, the structural consequences have been less well explored. Alkali metal cations, such as Na^+ and K^+, have been shown to stabilize single Pt and Au atoms, irrespective of whether the support is reducible or not[85,86]. DFT calculations for these SACs enabled the proposal of complex formulations of $(Au/Pt)O_y(OH)_z(Na/K)_x$, in which alkali metal cations are linked to the PGM centres through oxo ligands, where $x \leq 9$. In contrast, Na^+-modified Pt/Fe_3O_4 features $NaFeO_2$ surface species, which play a crucial role in stabilizing single Pt sites by forming Pt–O–Na–O–Fe linkages[87]. This result suggests that alkali metal cations interact with the support, serving as an 'interfacial chemical glue' to anchor the single Pt metal centres to the support.

SACs on other metals. When heteroatomic bonding between two metals is stronger than homoatomic bonding, it becomes possible, in principle, to have one metal atom (say, M1) isolated in an array of atoms of a second metal (say, M2). If M1 is the active metal, then the more inert M2 host will be present in higher concentrations (for example, $[M1]/[M2] < 10$) to ensure that M1 atoms do not find each other. These resultant bimetallic SAAs[31,37] often exhibit better catalytic performance than the individual elements[22]. So far, the SAA catalysts reported include PGMs alloyed with group 10 and 11 metals to give the intermetallics Pd–Au (REFS[88,89]), Pd–Ag (REF.[90]), Pd–Cu (REFS[37,91]), Pd–Zn (REF.[31]), Pd–In (REF.[92]) and Pt–Cu (REF.[93]), among others. Compared with random and/or disordered alloys, the SAA catalysts have unique properties owing to the isolation of atoms of one element. For example, SAAs exhibit unique selectivity in the hydrogenation of C≡C triple bonds because they bind the reduced C=C products only weakly. This weak π-bonding to alkenes also translates to these SAAs binding CO more weakly than do PGM NPs[31,37,90–93]. Thus, SAA catalysts are more CO-tolerant[94] — an important feature for a selective hydrogenation catalyst. It is noted that because of the strength of metal–metal heteroatomic bonding in SAAs, these systems are often more stable than oxide-supported or carbon-supported SACs. Compared with oxide-supported and carbon-supported SACs, SAAs may also benefit from the ensemble effect (geometric effect), electronic effect and strain effect, which are often observed in random alloy or intermetallic compounds.

Maximizing the activity per metal atom

We have noted that SACs can accelerate many types of reactions, ranging from typical thermochemical reactions to electrochemical and photochemical conversions. The benefits of SACs over other catalysts are multifarious

and may not come in the form of faster rates. For example, SACs are not always more catalytically active than their NP counterparts. Indeed, they might be completely inactive or serve only as a promoter or spectator in reactions, particularly ones that require two or more neighbouring metal atoms to activate a reactant. NPs will always be superior to SACs in such conversions. In general, while some SACs can have even orders of magnitude higher activity than their NP counterparts based on turnover frequency (TOF; moles of product formed per active metal atom per unit time), the reaction rate per overall catalyst mass is, in the case of SACs, at least one order of magnitude lower than that of supported NPs, because the former feature only low coverages of active atoms. Therefore, the practical utility of SACs is limited by our ability to decorate supports with high coverages of active single atoms. Only in this way can we maximize space–time yield (product yield per volume of catalyst per unit time). Towards this goal, many have experimented with new preparation approaches in addition to traditional wet-chemistry methods. For example, the photochemical reduction of $H_2[PdCl_4]$ on ethyleneglycol-decorated TiO_2 nanosheets affords a very stable Pd_1/TiO_2 SAC with a Pd loading of 1.5 wt%, a material that is an order of magnitude faster than commercial Pd/C for alkene hydrogenation[39]. In general, achieving high loadings of isolated single atoms while avoiding NP formation is nontrivial. However, by using alkali metal cations during the synthesis of a Pt/FeO_x hydrogenation catalyst, we have accessed a 'pseudo-SAC' with up to 2.16 wt% Pt (REF.[87]). Such high-density SACs maintain the exceptionally high TOF values possible with SACs but also have high space–time yields. We envisage that rapid advancements in synthetic chemistry and materials science will give us more controllable and practical syntheses of high-density SACs, examples of which are emerging in recent literature[40,42,79,95]. Studies aimed at increasing surface coverage are complemented by recent progress in maximizing the activity per metal atom. Selected examples illustrating how to increase this specific activity are described below.

CO oxidation, PROX, WGS and MSR. The WGS reaction and CO oxidation — including the preferential oxidation of CO (PROX) in the presence of H_2 — are among the most intensively studied reactions in which SACs are used. It has been well established that SACs on reducible oxide supports (for example, single PGM centres on FeO_x, CeO_2 or TiO_2) or Na^+-modified single PGM atoms on non-reducible oxides (for example, zeolites, carbon or SiO_2) are more active than their NP counterparts for the WGS reaction[49,85,86,95–97]. Indeed, for surfaces decorated with both single metal centres and NPs, the latter are often only spectators during the WGS reaction. In comparison, SACs are not always superior to NPs in CO oxidation, and the relative merits of each motif depend on a variety of factors[2,98,99]. A systematic study of CO oxidation and PROX reactions over single PGM atoms or NPs on reducible oxides showed that catalytic activity comes on a case-by-case basis. On one hand, Pt_1/FeO_x is 2–3 times more active than Pt NPs for both CO oxidation and PROX[2]; on the other hand, Ir_1/FeO_x and Rh_1/TiO_2 are considerably less active than their NP counterparts[51,100], while Au_1/FeO_x has activity comparable to that of its NP counterpart[48]. The catalytic activity for single atoms on the same FeO_x support follows the order $Au_1 > Pt_1 > Ir_1 \approx Rh_1$, with the strength of CO adsorption to these single atoms following the opposite trend. Further theoretical efforts are needed to elucidate the nature of these SAC reactivity trends[72]. However, discrepancies exist between theoretical and experimental results for SACs, perhaps reflecting the complicated chemistry at play. As we have noted, under reaction conditions, samples of M_1/FeO_x feature a support whose surface is dominated by Fe_3O_4, with the abundant oxygen vacancies and hydroxyl groups likely playing important roles in the oxidation reactions. Unfortunately, these surface features have not been considered in most theoretical treatments. Indeed, the reducible oxide support plays a vital role in low-temperature CO oxidation by either O_2 or H_2O (WGS) because the support provides reactive O atoms for the reaction[101]. Moreover, the presence of trace H_2O can facilitate CO oxidation, an effect that is much greater when a reducible oxide supports single atoms instead of NPs[102]. This H_2O dependence may account for the PROX reaction proceeding more rapidly than CO oxidation when using SACs on reducible oxides. In operando spectroscopy reveals that a surface lattice O atom of the FeO_x support directly participates in CO oxidation through a redox mechanism assisted by the single PGM atoms[103]. The importance of surface O atoms is also evident when studying Pt/CeO_2, which, although inferior to Pt/FeO_x, can have improved properties after steam treatment at 750 °C. It is thought that the treatment affords active surface lattice O atoms in the vicinity of Pt^{2+}, thereby increasing activity for low-temperature CO oxidation[104].

Methanol steam reforming (MSR; $CH_3OH + H_2O \rightleftharpoons CO_2 + 3H_2$) and aqueous-phase reforming of methanol (APRM) are important reactions to produce H_2 from liquid fuels. Like PROX and WGS reactions, MSR and APRM also involve H_2O dissociation ($H_2O \rightarrow H^* + OH^*$; the asterisks denote surface-bound species) and the reaction between adsorbed CO and OH ($CO^* + OH^* \rightarrow CO_2H^* \rightarrow CO_2 + H^*$). Both PROX and WGS reactions can be catalysed by single metal centres supported on reducible oxides, and one would expect MSR and APRM to also occur on the same type of SACs. Indeed, Au atoms on CeO_2 nanorods[105] and ZnO nanowires[106] are highly active for MSR. More interestingly, when Pt atoms are dispersed on α-MoC, the resulting Pt/α-MoC SAC exhibits unprecedented catalytic activity (TOF up to 18,046 h^{-1}) for APRM at 150–190 °C (REF.[107]). Such promising performance stems from the cooperation between single Pt atoms and the α-MoC support. Electron-deficient Pt sites are responsible for the adsorption and activation of CH_3OH, the α-MoC surface cleaves H_2O, and the reforming reaction occurs between the Pt atoms and α-MoC. The strong interaction between Pt and α-MoC greatly changes the electronic structure of the individual components, with charge transfer making the Pt atoms electron deficient and the interface between Pt and α-MoC electron rich. This has a substantial effect on

the adsorption of both reactants and intermediates to the SAC. This Pt_1/α-MoC system is quite different from most other SACs in that the individual support material and metal have similar catalytic properties when used separately. The success of the Pt_1/α-MoC SAC, in particular for reactions involving H_2O (MoC would be readily oxidized in H_2O if Pt were not present), will inspire the exploration of more SAC systems, including those with non-precious metals.

SACs in electrocatalysis and photocatalysis. Inspired by the nearly 100% utilization of metals in SACs and driven by the practical requirement for low-cost electrocatalysts, the application of SACs in electrochemical reactions is becoming an active research area[46,47,108]. Although the thermocatalytic activity depends only on the nature and number of active sites, electrocatalytic and photocatalytic reactions additionally require a catalyst with high electrical conductivity or light absorbance, respectively. These requirements are often met by using heteroatom-doped carbonaceous supports for electrocatalysis, while graphitic carbon nitride ($g\text{-}C_3N_4$) and other light-absorbing materials are preferred for photocatalysis. The two main types of SACs that have been investigated for electrocatalysis are the M–N–C SACs and PGM SACs. Members of the M–N–C class of materials are considered some of the most promising candidates to replace Pt in electrochemical reactions such as the ORR[109]. However, early reports of M–N–C described only materials in which not all the metal centres are atomically dispersed. Indeed, these systems feature metallic nanoparticles and large metal carbides in addition to M_1 single atoms. The presence of these larger species decreases the specific activity and selectivity and contributes to the already considerable challenges in identifying the catalytically active single metal sites.

Recent progress in synthetic routes and characterization methods for SACs have renewed our interest in the synthesis of atomically dispersed M–N–C electrocatalysts, including Co–N–C (REFS[42,75,78,82]), Fe–N–C (REFS[79–81]), Ni–N–C (REF.[77]) and Cu–N–C (REF.[76]) materials. For example, MOF-derived Co–N–C and Fe–N–C SACs are superior to commercial Pt/C catalysts for the ORR in alkaline electrolytes, giving rise to catalysis at half-wave potentials of 0.881 V and 0.900 V, respectively[42,79]. The high activity is attributed to the high rates at which single Co and/or Fe atoms transport electrons to adsorbed OH species. An alternative synthetic method is the pyrolysis of graphene oxide and $CoCl_2$ in NH_3 at 750 °C, which affords single Co atoms on N-doped graphene (Co–NG). This Co–NG SAC is highly active for the hydrogen evolution reaction (HER; $2H^+ + 2e^- \rightarrow H_2$) in both acidic and alkaline media, with this new and robust material having a TOF per metal atom higher than or similar to other non-precious metal HER catalysts[75]. Preparations can also make use of well-defined molecular complexes. Indeed, ball-milling first-row transition metal phthalocyanines with graphene nanosheets affords a series of composites with single metal sites that exhibit high activity and stability when used as counterelectrodes in dye-sensitized solar cells[78]. These materials are described as having metals bound to four N donor atoms, but this donor number can vary between two and six, with the exact nature of the active sites being unknown. This and many other studies lack in operando characterization of the oxidation state and the coordination environment of the single metal centres during the electrochemical reactions. Beyond the intrinsic activity of $M\text{–}N_x$ complex sites, the electrocatalytic performance of M–N–C SACs also depends on the pore structure and electrical conductivity of the carbon materials, which affect both mass and electron transport.

Besides the exploration of base metal M–N–C SACs for electrocatalysis, ongoing efforts in SAC research are aimed at downsizing PGMs to single atoms to maximize the utilization efficiency of PGMs and perhaps make them economically sustainable. For example, single Pt atoms deposited on N-doped graphene nanosheets using ALD exhibit notably high activity and stability for the HER in acidic media. The new materials give rise to a mass activity 7.8 times higher than their Pt NP counterpart and 37.4 times higher than the commercial Pt/C catalyst[110]. The XAS and DFT analyses suggest that the superior activity of the Pt SAC arises from the partially unoccupied Pt 5*d*-like orbitals, which favour both adsorption of H and desorption of H_2. A related Pt SAC on N-doped carbon black is highly active for the $4e^-$ ORR in an acidic single cell, giving a power density of 680 mW cm^{-2} at a Pt loading of only 0.09 mg_{Pt} cm^{-2} (REF.[111]). This result is surprising given that the $4e^-$ required to cleave O_2 can apparently come from only one Pt atom[33]. DFT calculations revealed that the single Pt atoms are anchored to single pyridinic N atoms to give PtN active sites that can activate O_2 but are poor binding sites for CO.

We have noted the profound catalytic effects of introducing metals into N-doped carbon, and it so happens that doping single Pt and Co atoms onto 2D MoS_2 can have similar consequences. Doping transforms the inert in-plane S atoms near the single-atom dopants into highly active sites for the HER. Introducing only 1.7 wt% Pt can lower the HER overpotential by about 60 mV relative to bare MoS_2 (REF.[112]).

The reactivity of supported single metal atoms has recently been applied to photocatalytic conversions. Ideal support materials must absorb solar light and also provide binding pockets to stabilize the single atoms. In this regard, $g\text{-}C_3N_4$ is a promising candidate owing to its high stability, excellent visible-light absorption and capability to bind noble metal centres through N donor atoms. Depositing single Pt atoms on $g\text{-}C_3N_4$ increases the photocatalytic HER activity by 50-fold compared with $g\text{-}C_3N_4$, and the TOF per Pt atom of $Pt/g\text{-}C_3N_4$ is about eight times higher than that of $Pt\ NP/g\text{-}C_3N_4$ (REF.[70]). The presence of the Pt atoms changes the surface trap states of $g\text{-}C_3N_4$ and promotes photogenerated electron–hole separation. Beyond the HER, DFT calculations predict $Pt/g\text{-}C_3N_4$ and $Pd/g\text{-}C_3N_4$ SACs to also be highly active for CO_2 photoreduction to CH_4 and HCO_2H, respectively[71]. Here, $g\text{-}C_3N_4$ delivers H atoms to the PGM atoms, which serve as the active sites for CO_2 reduction.

Tuning selectivity

In any catalytic process, selectivity is at least as important as activity. Reactions that proceed with low selectivity require potentially complicated and energy-intensive downstream separation processes that will likely cause environmental problems. The uniformly dispersed, strongly anchored and typically electron-deficient nature of SACs means that we have access to well-defined tuneable systems. Indeed, one can tune reaction selectivity either by changing the mode and strength of the reactant, intermediate and/or product adsorption or by changing the reaction pathway. The tuning of SACs has been to the benefit of many reactions, and selective hydrogenation in particular has become one of the success stories involving SACs.

Hydrogenation of substituted nitroarenes. The chemoselective hydrogenation of substituted nitroarenes is an important process in the manufacture of agrochemicals, pharmaceuticals and dyes. This selective conversion of a nitro group into an amino group has been studied using various heterogeneous nanocatalyst systems, such as supported Au, Ag and PGMs as well as bimetallic NPs. Superior to these traditional catalysts are Pt/FeO_x SACs, and at Pt loadings of just 0.08 wt%, one has a material with outstanding performance in terms of activity, chemoselectivity and substrate scope[30]. For example, in the hydrogenation of 3-nitrostyrene, Pt/FeO_x SACs give rise to a TOF of ~1,500 h^{-1}, and 3-aminostyrene is formed with a selectivity close to 99%. Moreover, these SACs exhibit good stability and can easily be recovered by magnetic separation. The high chemoselectivity when hydrogenating this and other nitroarenes arises because the $–NO_2$ group binds more strongly to the catalyst than do other reducible groups, such as C=C, C≡C, C=O or –Cl. It is proposed that the isolated cationic Pt centres bind the hard partially anionic O atoms of the $–NO_2$ group in preference to the other less polar reducible groups. The crucial role of isolated cationic centres can be further taken advantage of by introducing alkali metal cations to Pt/FeO_x SACs with high Pt loadings, thereby obtaining >20-fold mass activity with similarly high TOF values and chemoselectivities[87].

Aside from the single cationic metal centres in SACs, the support is also important for directing the chemoselective hydrogenation of nitroarenes. When 4-nitrophenol is reduced over subnanometre Pd clusters on porous CeO_2 nanorods, surface defects — O vacancies on the reduced CeO_2 — are necessary for the preferential adsorption of $–NO_2$ groups[113]. FTIR spectra and DFT calculations suggest that the two O atoms of the $–NO_2$ group coordinate strongly to three Ce centres adjacent to an O vacancy. The subnanometric or even mononuclear metal sites are sterically hindered from binding such large molecules. Therefore, it appears that the high catalytic activity of this catalyst is associated with both the dispersion of the metal sites and the concentration of surface O vacancies, while the chemoselectivity is mainly governed by the single-atom dispersion of the active metal.

Hydrogenation of alkynes and dienes. The selective hydrogenation of acetylene to ethylene is industrially important because it contributes to the high purity of the ethylene feedstock, which is necessary for polymerizations. The most desirable catalysts hydrogenate acetylene to ethylene but do not mediate over-hydrogenation to ethane even in ethylene-rich streams. Industrially, the reaction is carried out over a supported Pd catalyst with promoters, and the Pd loading can be as low as several hundreds of ppm. Such low-loading Pd catalysts may contain isolated Pd centres, although no experimental characterization data exist to confirm their presence. Recent developments in advanced synthetic and characterization methods for SACs have enabled the study of supported Pd SACs for the selective hydrogenation of C≡C bonds, dienes and other unsaturated systems[31,37,41,69,90–93]. Comparing the performances of Pd SACs with those of NPs, we find that single Pd centres — no matter what the neighbouring atoms are (Pd can be supported on different substrates or be part of an SAA) — are crucial for high activity and selectivity. The high selectivities (>90%) and conversions (>90%) achieved using Pd SACs cannot be obtained using commercial catalysts or Pd NPs. The superior performance of Pd SACs is associated with the absence of Pd–Pd bonding; such multinuclear sites would strongly bind ethylene and catalyse its further hydrogenation to ethane.

The selective hydrogenation of acetylene has also been studied using a model single-crystal SAA catalyst: single Pd atoms on Cu(111)[37]. The single Pd atoms are sufficiently active to split H_2, with the resulting H atoms spilling over to the Cu(111) surface and then desorbing easily to combine with acetylene. The Pd atoms thus allow the facile dissociation of H_2 yet bind the resulting H atoms weakly. These mechanistic proposals and the high selectivity are backed up by microcalorimetric and DFT studies, which provide strong evidence that the single Pd atoms are responsible for H_2 activation, while acetylene adsorbs on the support or more inert alloying metal. Finally, hydrogenation occurs on the surface adjacent to the single Pd atoms. In the case of Pd/Zn SAAs, the Pd–Zn–Pd fragments bind acetylene and ethylene, although they do so by different modes. The spatial arrangement of Pd atoms allows for moderately strong σ-bonding of acetylene, which bridges two neighbouring Pd sites. In contrast, ethylene cannot bridge the atoms and only participates in weak π-bonding with an isolated Pd atom[31]. Lastly, we note that Pt-based SAAs are also useful for hydrogenations; for example, a Pt–Cu SAA (Pt/Cu < 1/100) is active for the selective hydrogenation of 1,3-butadiene to butenes under mild conditions. The high selectivity (>95%) at nearly 100% conversion further demonstrates the power of SACs in these types of reactions[93].

Hydrogenation of carbon dioxide. The hydrogenation of CO_2 has been extensively studied and is of interest in the context of renewable fuels[114]. This reaction can be catalysed by supported PGM materials, in which case product selectivity is very sensitive to the size of the

PGM active sites. Single atoms of Pd (REF.[115]), Ru (REF.[116]) and Rh (REF.[32]) are highly selective for the formation of CO as part of the reverse WGS (r-WGS) reaction. In contrast, 3D particles of these metals give CH_4 as the major product. As we have noted in related SAC versus NP comparisons, SACs selectively give CO as the end product because it is easily released from the single metal site and relatively few H atoms are present to further reduce CO. In contrast, NPs hold on to CO, which bridges electron-rich metal centres in a stable bonding arrangement. CO can then undergo hydrogenation by combining with the many H atoms present on the NP surface. Another way to rationalize the result is to consider the strong metal–support interaction (SMSI), whereby single metal centres are cationic on account of electron transfer to reducible supports[117]. This interaction occurs to the maximum degree when the metal is present as single atoms. The outstanding performance of SACs in the r-WGS reaction is perhaps not surprising given their unique activity in the WGS reaction. The fact that SACs do not induce CO or CO_2 methanation may be of practical importance in WGS reactions conducted in the presence of CO_2, when one would want to avoid consumption of the H_2 that has been produced[97].

Along with the thermal reduction of CO_2, the electrochemical reduction of CO_2 is also a promising method to produce fuels and value-added chemicals. The challenges associated with manipulating the selectivity can be met using SACs, including SAAs composed of single Rh, Co or Ir atoms diluted by Au or Ag metal, or single metal atoms supported on graphene or carbides. Such SACs, according to DFT calculations, can be highly selective for CO_2 reduction over the HER, which can be ascribed to the surface adsorption of CO_2 reduction intermediates (for example, $*CO_2H$) being stronger than that of H atoms. Once more, the success of SACs stems from the active metal atoms being cationic and not bonding to each other[118–123]. SACs do not obey the typical scaling relationships associated with the binding of intermediates to bulk transition metals, such that the selectivities of SACs can be tuneable and quite different from that of a bulk metal. Data for Cu–Sn SAA[121] and Ni–N–C (REFS[122,123]) catalysts show them to be highly selective for the $2H^+/2e^-$ electroreduction of CO_2 to CO, with Faradaic efficiencies for CO formation exceeding 90%. In particular, the isolated Ni(I) centres in N,S-doped graphene exhibit high activity (TOF 14,800 h^{-1} at an overpotential of 0.61 V), selectivity (97% Faradaic efficiency for CO) and stability (only 2% loss of activity after 100 h of electrolysis)[123]. More challenging than the electroreduction of CO_2 to CO are conversions affording C2 chemicals — demanding reactions that involve C–C coupling. Single Fe(II) sites on N-doped carbon are active and selective for the formation of CH_3CO_2H (selectivity of 61% and Faradaic efficiency of 97.4%)[124], exemplifying the promise of SACs in CO_2 reduction reactions.

Reduction of oxygen to hydrogen peroxide. There is great interest in catalysing the ORR and doing so in a way to selectively promote either a $4e^-$ ($4H^+ + 4e^- + O_2 \rightarrow 2H_2O$) or $2e^-$ ($2H^+ + 2e^- + O_2 \rightarrow H_2O_2$) pathway. The former half-reaction is preferred for energy applications because it results in the most exergonic overall reaction. However, there is also interest in the latter half-reaction, and although H_2O_2 production in a H_2/O_2 fuel cell has been known since 1990, problems arise in that the use of alkaline electrolytes is undesirable because H_2O_2 undergoes decomposition under basic conditions. Furthermore, there are concerns about the stability of hydroxide-conducting polymeric membranes and the poor H_2O management[125]. Thus, it is desirable to produce H_2O_2 under neutral or acidic conditions, despite these posing a great challenge for the development of highly active, selective and stable cathodic ORR catalysts. SACs featuring strongly anchored isolated metal centres are expected to provide new opportunities towards this goal. The absence of metal–metal bonding in SACs means that these catalysts do not have the reducing equivalents to effect reduction of O_2 to H_2O, a reaction that generally requires at least two adjacent active metal sites. However, SACs can reduce O_2 to H_2O_2, and they do so selectively because the $4e^-$ pathway is unavailable. In this way, the utilization of SACs allows for the selective production of H_2O_2 together with the production of electric power.

It turns out that by moving from a bulk catalyst to a SAC, one can deliberately steer the ORR from a $4e^-$ pathway to a $2e^-$ pathway. This effect can be understood by studying the SAA catalyst $PtHg_4$, an intermetallic compound in which Pt atoms are surrounded by Hg atoms[126]. This SAA catalyst exhibits high Faradaic efficiency for H_2O_2 production (96% between 0.2–0.4 V) under acidic conditions. Moreover, the catalyst is very stable, with no measurable losses in H_2O_2 production activity after cycling the potential between 0.05 V and 0.8 V 8,000 times in O_2-saturated electrolyte. A more active and less expensive catalyst is the related Pd–Hg SAA, which gives rise to a mass activity five times higher than that of Pt–Hg/C and more than two orders of magnitude higher than that of the state-of-the-art Au/C material at a 50 mV overpotential[127]. SAAs based on Hg as the more inert metal are promising, but the ability of Hg to form bonds to other metals and stabilize single atoms comes at the price of toxicity and environmental concerns. A safer approach makes use of an incipient wetness impregnation method, whereby aqueous $H_2[PtCl_6]$ is evaporated onto TiN and exposed to H_2 in order to reduce the Pt(IV) centres. The atomic dispersion of Pt sites was ensured by using only 0.35 wt% Pt (REF.[33]). For the ORR, the mass activity per Pt atom in the Pt/TiN SAC is one order of magnitude higher than the corresponding value for Pt NPs, and the H_2O_2 selectivity reaches 65%. Decreasing the Pt content can further increase the selectivity of H_2O_2 to 90%, but at the cost of lower catalytic currents. Once more, this brings us to the challenge of preparing a SAC with a high spatial density of active sites. A high density of active metal sites can be had if there is also a high density of heteroatoms, as is the case with S-doped carbon prepared by CVD of acetylene and H_2S on a zeolite template. After etching away the zeolite with HCl/HF solution[73], the resulting carbon material features up to 17 wt% S in the curved 3D networks of graphene nanoribbons. The high density of these soft donor atoms enables the material to

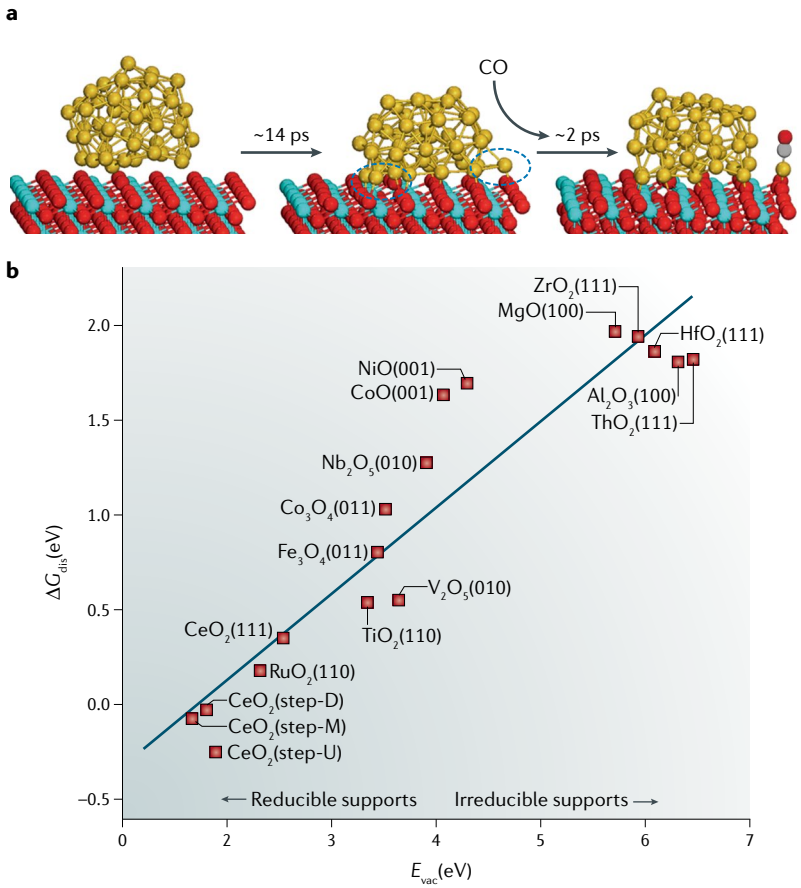

Fig. 5 | **Au clusters on oxides can act as dynamic single-atom catalysts for CO oxidation. a** | Snapshots from a molecular dynamics simulation of a CeO_2-supported Au_{50} cluster show that a single Au atom can dissociate from the cluster to bind CO. **b** | The Gibbs free energy change for Au cluster disintegration (ΔG_{dis}) can be plotted against the energy associated with the formation of support vacancies (E_{vac}). The more reducible the support, the more stable the single Au centres are after dissociating from an Au cluster. Part **a** is reproduced from REF.[130], CC-BY-4.0. Part **b** is adapted with permission from REF.[131], American Chemical Society.

host single Pt metal centres at relatively high loadings (5 wt%). The Pt centres exist as Pt^{2+} ions that are proposed to be bonded to two thiolate S atoms and two thiophene-like S atoms in square-planar charge-neutral active sites. This catalyst reduces O_2 to H_2O_2 at selectivities up to 96% without considerable loss of activity even over extended electrolysis times.

Dynamics of SACs

The stability of SACs always comes into question because single atoms, if bound only weakly to a support, are susceptible to aggregation during pre-activation and reaction processes. A growing body of evidence suggests that single atoms anchored to a surface through strong covalent bonds can be more stable than their NP counterparts and are even resistant to sintering during reactions at high temperatures[34–36,48,104]. Some reports suggest that SACs can survive intact under the harsh hydrothermal conditions used for biomass conversions[128].

The structures of SACs may change during catalysis as a result of well-known restructuring phenomena induced by chemical reactions and/or high temperatures. Understanding the dynamism of SACs under reaction conditions is important, especially given the recent finding that NPs can dynamically convert into single-atom active centres during catalysis, a phenomenon termed dynamic single-atom catalysis[129–131]. A series of ab initio molecular dynamics simulations and static DFT studies of CO oxidation on reducible-oxide-supported Au NPs revealed that CO adsorption on Au apices could afford Au(I)CO complexes that migrate across the NP surface or even onto nearby sites at the NP–support interface[130,131] (FIG. 5a). These mononuclear complexes have a crucial role in the catalytic mechanism, and their dynamism is evident in their reincorporation into NPs following catalysis. Moreover, the dynamics of CO-mediated formation of single Au atoms are strongly dependent on the support; more reducible supports afford stable Au centres that are more positively charged and are poorer binding sites for π-acids such as CO (FIG. 5b). These theoretical proposals suggesting the importance of Au(I)CO complexes have been supported by subsequent experiments[132]. Moreover, even Cu(111) — the most stable surface of a Cu crystal — has been shown to undergo etching and break into nanoclusters upon exposure to CO, thereby affording catalytically active sites for H_2O splitting[133].

The mobility of single Pt atoms on $Fe_3O_4(001)$ increases when exposed to CO owing to the formation of Pt(CO) species, which eventually agglomerate into subnanometre Pt clusters[134]. Although removing CO from the surface leads to partial redispersion back to single Pt atoms, this study suggests that sequential CO adsorption and desorption steps could result in the sintering of single-atom species. The occurrence of this irreversible deleterious process further highlights our need to conduct in operando and post-reaction characterization of SACs. Such CO-induced formation of subnano Pt clusters is in contrast to the dynamic formation of single Au atoms[129–132], reflecting the complicated nature of heterogeneous catalysis, even when the catalytic metal atom sites are uniformly mononuclear. Similar to the presence of absorbed CO, adsorbed H atoms on Pt SACs enhance Pt diffusivity by a factor of 500, resulting in sintering of the Pt atoms[135]. Contrary to the reducing atmosphere, a lean-H_2 reaction atmosphere was found to promote the disintegration of Rh nanoparticles into single atoms during CO_2 hydrogenation, leading to greater CO selectivity[32]. The ubiquity of dynamic behaviour in heterogeneous catalysis highlights the importance of in operando characterization techniques[136]. The application of these techniques to dynamic single-atom catalysis is still in its infancy, and more in operando data and computational modelling will be needed to elucidate the interconversions between nanoparticles and single atoms during catalysis.

Bridging homo- and heterogeneous catalysis

Conceptually speaking, the often well-defined mononuclear sites in SACs represent a merger of homogeneous and heterogeneous catalysis. We now present two examples in which we compare the activities of SACs with closely related homogeneous and heterogeneous systems. Although many such comparisons exist, we

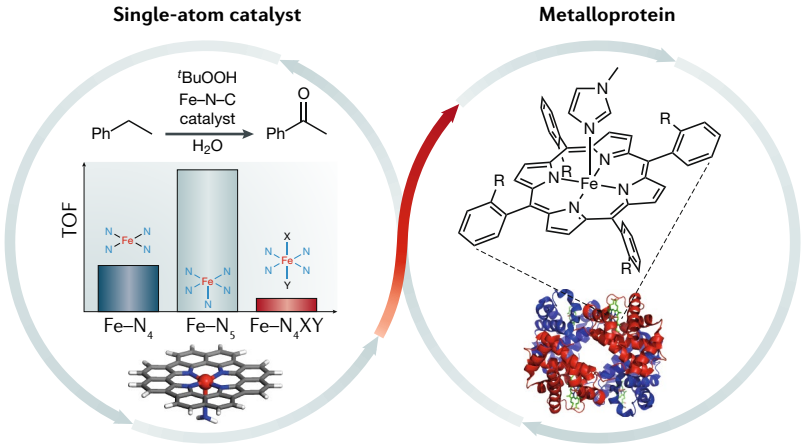

Fig. 6 | **A single-atom Fe–N–C oxidation catalyst and related metalloprotein.** Characterization of a Fe–N–C single-atom catalyst reveals four different Fe–Nx ($x = 2–4$) active site structures, each giving rise to a different turnover frequency (TOF) for ethylbenzene oxidation to acetophenone. The Fe–N_5 sites exhibit the highest activity. Haemoglobin makes use of a similar Fe–N_5 site to bind O_2. A simplified porphyrinatoiron complex is also depicted, with the inclusion of a 1-methylimidazole ligand leaving one vacant Fe coordination site for substrate binding. The left portion is adapted with permission from REF.[84], American Chemical Society.

chose a study on the industrially relevant hydroformylation reaction conducted over supported single Rh atoms as well as a study of organic transformations over atomically dispersed M–N–C catalysts.

The hydroformylation of olefins is arguably the most important industrial process involving homogeneous catalysis. The propensity of organic ligands, such as triarylphosphines, to undergo oxidation or other modes of decomposition and the difficulties associated with catalyst recovery have motivated the search for heterogeneous catalysts with comparable activities and selectivities to state-of-the-art homogeneous catalysts[137]. Single Rh atoms supported on ZnO nanowires exhibit high activity for the hydroformylation of olefins, with the turnover number (TON) for styrene conversion reaching 40,000 under mild reaction conditions (0.8 MPa CO, 0.8 MPa H_2 and 100 °C), which is even higher than that observed using [$RhCl(PPh_3)_3$] (Wilkinson's catalyst)[138]. Another notable advantage of the Rh/ZnO SAC is the almost 100% chemoselectivity for olefin hydroformylation over hydrogenation, a result attributed to the absence of Rh–Rh bonding in the SAC. Unfortunately, the Rh/ZnO SAC exhibits poor selectivity with respect to linear and branched aldehydes, with the reason for this yet to be understood. Similarly, a Rh/CoO SAC shows excellent activity (TOF reaching 2,065 h^{-1}) in the hydroformylation of propene, affording butyraldehyde in high selectivity (94.4%) and being stable during multiple catalytic experiments[139]. Both examples demonstrate that Rh SACs free of organic ligands can exhibit activity and selectivity comparable to those for the homogeneous phosphine-ligated Rh catalyst. In this regard, we can view the solid supports as robust ligands that tune the electronic structure of isolated Rh centres. For example, Rh centres in the Rh/ZnO SAC are close to being metallic (charge neutral), while they are in the +III oxidation state in the case of Rh/CoO. The different electronic structures of Rh in the two catalysts are reflected in their hydroformylation performance: Rh/ZnO is nonselective, while Rh/CoO is highly selective towards linear aldehyde products. Moreover, DFT calculations indicate a reconstruction of Rh single atoms during the reactions catalysed by Rh/CoO, facilitating the adsorption and activation of reactants[139]. This reconstruction or regeneration of single atom sites is analogous to processes operative in homogeneous catalysis.

Moving to M–N–C SACs, we note that these species have, owing to their active sites being similar to (and often derived from) metal complexes of N-donor macrocycles, many features in common with metalloenzymes. In this way, one also can view M–N–C SACs as having properties characteristic of both heterogeneous and homogeneous catalysts[140]. M–N–C SACs exhibit promising activities for a variety of organic transformations typically catalysed by homogeneous analogues, although the active site structures of the latter are far better understood[141]. For example, in haemoglobin, the central Fe ion is bound to four N atoms in a plane, with one apical position being occupied by a His ligand. The coordinatively unsaturated Fe site can reversely bind O_2 (FIG. 6, right). Reproducing such a FeN_5 structure in a SAC can be achieved by the pyrolysis of $Fe(OAc)_2$/phen/MgO mixtures, as we noted above[84]. The resultant catalysts exhibited high activity and excellent selectivity for the oxidation of C–H bonds in a broad scope of substrates. The four different Fe–N_x structures in the atomically dispersed Fe–N–C catalyst — FeN_4, high-spin FeN_6, low-spin FeN_6 and intermediate-spin Fe–N_5 — have different ethylbenzene oxidation activities (intermediate-spin Fe–N_5 ≫ Fe–N_4 ≫ high-spin Fe–N_6 ≫ low-spin Fe–N_6; FIG. 6, left). The activity of the Fe–N_5 structure, which is at least one order of magnitude higher than that of Fe–N_6 sites, reflects the importance of coordination unsaturation, which is of course also essential to the O_2-transport properties of haemoglobin. Unfortunately, the Fe-N-C SAC is not structurally uniform, and the Fe–N_5 active sites are also the least abundant. Coordination unsaturation is also important in the functioning of traditional heterogeneous catalysts, in which the edge or corner sites are usually believed to be the most reactive sites, despite comprising only a small fraction of the atoms when relatively large particles are used. Overall, there is a long way to go before we can truly bridge homogeneous and heterogeneous catalysis. Only when the latter can proceed over SACs with uniform and well-defined active sites can we truly begin to draw parallels.

Conclusions and future directions

Research on SACs has emerged as a new frontier in heterogeneous catalysis in the past several years. In contrast to supported metal NP or nanocluster catalysts, in which metal–metal bonding between like atoms dominates the chemistry, the present catalysts feature atomically dispersed metal centres — no homoatomic metal–metal bonds are present, and the metal atoms are attached to the support surface through either heteroatoms, in the case of SACs, or other metals, in the case of SAAs. These heteroatomic bonds can be polar and result in substantial charge transfer from the active metal to the support, affording electron-deficient single metal sites.

A theme we have stressed here is that absence of homoatomic metal–metal bonding and the cationic character of metals in SACs give rise to catalytic behaviour very different from that of NPs and bulk metals.

The term SAC simply emphasizes that each active site features only one active metal, even though these metals, while being isolated from each other, are anchored to a support through a variety of interactions. Tuning these interactions then becomes the most important way in which we can engineer SACs. The single metal sites in SACs more or less resemble the peripheral atoms at the NP–support interface of supported NP catalysts. In this aspect, SACs can be considered as model systems for these more complicated and less well-defined catalysts. The surface chemistry of the support has a substantial influence on the geometric and electronic properties of metal atoms attached to it. On oxide supports such as Fe_2O_3, CeO_2 or TiO_2, single atoms are stabilized by coordinating to surface oxo ligands. When on (or in) N-doped or S-doped carbon supports, the single metal atoms form ionic or covalent bonds to the anionic or neutral heteroatoms, respectively. The surface of a support can be modified in many ways; for oxides, this may involve engineering the size, shape and vacancy distribution, while for carbon materials, doping represents an easy way to include donor atoms and modulate electronic structure. Only through judicious tuning of a support will we arrive at desirable materials for high-density, thermally stable SACs.

Potentially every isolated metal centre in a SAC is accessible to reactants, and if a 100% metal atom utilization can be combined with a high coverage of reactive sites, then we would have a highly efficient catalyst. The isolated and cationic nature of supported single metal centres is key to their activity and selectivity in a variety of reactions. In particular, SACs exhibit exceptional selectivities in a variety of hydrogenation reactions, and such systems will likely attract more attention as practical applications come within reach. The high selectivity of many SACs is thought to arise from the uniform structure of SAC active centres and the metal–support interactions that are unique to these systems. In principle, reaction pathways that require two nearby active metal atoms are not possible. This unique property of SACs affects selectivity, as does changing the mode of adsorption and activation or the strengths with which the single metal centres bind reactants, intermediates and products.

Although heterogeneous catalysis studies suggest that isolated metal atoms are of broad mechanistic importance, the development of SACs is still in its infancy, and the field has become mainstream only in the past six years (roughly coincident with the SAC term being coined). An analytical problem remains in that we have yet to fully characterize the active centres in the vast majority of SACs. Fundamentally, we face other problems in our study of SACs. First, the non-uniformity of support materials means that not all of the single metal centres in SACs are equally accessible or equally active. Second, single metal centres do not perform catalysis alone; indeed, some of the reaction steps may occur at the surrounding support atoms. Then, we must ask ourselves what we consider to be the true active site. Third, little experimental evidence is available regarding the dynamic behaviour of SACs during catalysis. Tackling these fundamental questions requires in operando atomic-resolution and highly surface-sensitive spectroscopic techniques[98,124,136,142].

Industrial applications demand a high coverage of single atoms on robust supports. If each metal atom is highly active, we then have desirable product yields per volume or mass of catalyst. Meanwhile, single atoms can also be considered as the smallest building blocks to construct catalysts with structurally well-defined low-nuclearity metal active centres, which may take the form of a so-called single-cluster catalyst (SCC)[58,143] such as a dimer[144], trimer[145] or larger metal cluster. These well-defined (M_n/support) SCCs will likely contribute to sustainable chemical processes in the near future. The rapid development of single-atom catalysis in recent years suggests that it is not unreasonable to expect speedy access to robust SACs with high stability, selectivity and activity for industrially important reactions. More exciting surprises in the development of SACs as tuneable catalysts are undoubtedly just around the corner[146,147].

Published online 24 May 2018

1. Ye, R., Hurlburt, T. J., Sabyrov, K., Alayoglu, S. & Somorjai, G. A. Molecular catalysis science: perspective on unifying the fields of catalysis. *Proc. Natl Acad. Sci. USA* **113**, 5159–5166 (2016).
2. Qiao, B. et al. Single-atom catalysis of CO oxidation using Pt_1/FeO_x. *Nat. Chem.* **3**, 634–641 (2011).
3. Taylor, H. S. A theory of the catalytic surface. *Proc. R. Soc. Lond. A* **108**, 105–111 (1925).
4. Rooney, J. J. & Webb, G. The importance of π-bonded intermediates in hydrocarbon reactions on transition metal catalysts. *J. Catal.* **3**, 488–501 (1964).
5. Patterson, W. R. & Rooney, J. J. Single atom sites and hydrocarbon reaction mechanisms. *Catal. Today* **12**, 113–129 (1992).
6. Böhme, D. K. & Schwarz, H. Gas-phase catalysis by atomic and cluster metal ions: the ultimate single-site catalysts. *Angew. Chem. Int. Ed.* **44**, 2336–2354 (2005).
7. Kirlin, P. S. & Gates, B. C. Activation of the C–C bond provides a molecular basis for structure sensitivity in metal catalysis. *Nature* **325**, 38–40 (1987).
8. Vidal, V., Théolier, A., Thivolle-Cazat, J. & Basset, J.-M. Metathesis of alkanes catalyzed by silica-supported transition metal hydrides. *Science* **276**, 99–102 (1997).
9. Copéret, C., Chabanas, M., Saint-Arroman, R. P. & Basset, J.-M. Homogeneous and heterogeneous catalysis: bridging the gap through surface organometallic chemistry. *Angew. Chem. Int. Ed.* **42**, 156–181 (2003).
10. Serna, P. & Gates, B. C. Molecular metal catalysts on supports: organometallic chemistry meets surface science. *Acc. Chem. Res.* **47**, 2612–2620 (2014).
11. Bayram, E. et al. Agglomerative sintering of an atomically dispersed Ir-1/Zeolite Y catalyst: compelling evidence against Ostwald ripening but for bimolecular and autocatalytic agglomeration catalyst sintering steps. *ACS Catal.* **5**, 3514–3527 (2015).
12. Serna, P., Yardimci, D., Kistler, J. D. & Gates, B. C. Formation of supported rhodium clusters from mononuclear rhodium complexes controlled by the support and ligands on rhodium. *Phys. Chem. Chem. Phys.* **16**, 1262–1270 (2014).
13. Serna, P. & Gates, B. C. A bifunctional mechanism for ethene dimerization: catalysis by rhodium complexes on Zeolite HY in the absence of halides. *Angew. Chem. Int. Ed.* **50**, 5528–5531 (2011).
14. Asakura, K., Nagahiro, H., Ichikuni, N. & Iwasawa, Y. Structure and catalytic combustion activity of atomically dispersed Pt species at MgO surface. *Appl. Catal. A Gen.* **188**, 313–324 (1999).
15. Li, Z. Y. et al. Three-dimensional atomic-scale structure of size-selected gold nanoclusters. *Nature* **451**, 46–48 (2008).
16. Kaden, W. E., Wu, T., Kunkel, W. A. & Anderson, S. L. Electronic structure controls reactivity of size-selected Pd clusters adsorbed on TiO_2 surfaces. *Science* **326**, 826–829 (2009).
17. Vajda, S. et al. Subnanometre platinum clusters as highly active and selective catalysts for the oxidative dehydrogenation of propane. *Nat. Mater.* **8**, 213–216 (2009).
18. Abbet, S. et al. Acetylene cyclotrimerization on supported size-selected Pd*n* clusters ($1 \le n \le 30$): one atom is enough. *J. Am. Chem. Soc.* **122**, 3453–3457 (2000).
19. Fu, Q., Saltsburg, H. & Flytzani-Stephanopoulos, M. Active nonmetallic Au and Pt species on ceria-based water-gas shift catalysts. *Science* **301**, 935–938 (2003).
20. Zhang, X., Shi, H. & Xu, B.-Q. Catalysis by gold: isolated surface Au^{3+} ions are active sites for selective hydrogenation of 1,3-butadiene over Au/ZrO_2 catalysts. *Angew. Chem. Int. Ed.* **44**, 7132–7135 (2005).
21. Hackett, S. F. J. et al. High-activity, single-site mesoporous Pd/Al_2O_3 catalysts for selective aerobic oxidation of allylic alcohols. *Angew. Chem. Int. Ed.* **46**, 8593–8596 (2007).

22. Yang, X.-F. et al. Single-atom catalysts: a new frontier in heterogeneous catalysis. *Acc. Chem. Res.* **46**, 1740–1748 (2013).
23. Thomas, J. M., Raja, R. & Lewis, D. W. Single-site heterogeneous catalysts. *Angew. Chem. Int. Ed.* **44**, 6456–6482 (2005).
24. Liu, J. Aberration-corrected scanning transmission electron microscopy in single-atom catalysis: probing the catalytically active centers. *Chin. J. Catal.* **38**, 1460–1472 (2017).
25. Ogino, I. X-Ray absorption spectroscopy for single-atom catalysts: critical importance and persistent challenges. *Chin. J. Catal.* **38**, 1481–1488 (2017).
26. Asokan, C., DeRita, L. & Christopher, P. Using probe molecule FTIR spectroscopy to identify and characterize Pt-group metal based single atom catalysts. *Chin. J. Catal.* **38**, 1473–1480 (2017).
27. Parkinson, G. S. Unravelling single atom catalysis: the surface science approach. *Chin. J. Catal.* **38**, 1454–1459 (2017).
28. Hutchings, G. J. Vapor phase hydrochlorination of acetylene: correlation of catalytic activity of supported metal chloride catalysts. *J. Catal.* **96**, 292–295 (1985).
29. Malta, G. et al. Identification of single-site gold catalysis in acetylene hydrochlorination. *Science* **355**, 1399–1403 (2017).
30. Wei, H. et al. FeO*x*-supported platinum single-atom and pseudo-single-atom catalysts for chemoselective hydrogenation of functionalized nitroarenes. *Nat. Commun.* **5**, 5634 (2014).
31. Zhou, H. et al. PdZn intermetallic nanostructure with Pd–Zn–Pd ensembles for highly active and chemoselective semi-hydrogenation of acetylene. *ACS Catal.* **6**, 1054–1061 (2016).
32. Matsubu, J. C., Yang, V. N. & Christopher, P. Isolated metal active site concentration and stability control catalytic CO_2 reduction selectivity. *J. Am. Chem. Soc.* **137**, 3076–3084 (2015).
33. Yang, S., Kim, J., Tak, Y. J., Soon, A. & Lee, H. Single-atom catalyst of platinum supported on titanium nitride for selective electrochemical reactions. *Angew. Chem. Int. Ed.* **55**, 2058–2062 (2016).
34. Qiao, B. et al. Highly efficient catalysis of preferential oxidation of CO in H_2-rich stream by gold single-atom catalysts. *ACS Catal.* **5**, 6249–6254 (2015).
35. Jones, J. et al. Thermally stable single-atom platinum-on-ceria catalysts via atom trapping. *Science* **353**, 150–154 (2016).
36. Zhang, Z. et al. Thermally stable single atom Pt/m-Al_2O_3 for selective hydrogenation and CO oxidation. *Nat. Commun.* **8**, 16100 (2017).
37. Kyriakou, G. et al. Isolated metal atom geometries as a strategy for selective heterogeneous hydrogenations. *Science* **335**, 1209–1212 (2012).
38. Liu, W. et al. Single-atom dispersed Co–N–C catalyst: structure identification and performance for hydrogenative coupling of nitroarenes. *Chem. Sci.* **7**, 5758–5764 (2016).
39. Liu, P. et al. Photochemical route for synthesizing atomically dispersed palladium catalysts. *Science* **352**, 797–800 (2016).
40. Wei, H. et al. Iced photochemical reduction to synthesize atomically dispersed metals by suppressing nanocrystal growth. *Nat. Commun.* **8**, 1490 (2017).
41. Yan, H. et al. Single-atom Pd_1/graphene catalyst achieved by atomic layer deposition: remarkable performance in selective hydrogenation of 1,3-butadiene. *J. Am. Chem. Soc.* **137**, 10484–10487 (2015).
42. Yin, P. et al. Single cobalt atoms with precise N-coordination as superior oxygen reduction reaction catalysts. *Angew. Chem. Int. Ed.* **55**, 10800–10805 (2016).
43. Liu, J. Catalysis by supported single metal atoms. *ACS Catal.* **7**, 34–59 (2017).
44. Schwarz, H. Mênage-à-trois: single-atom catalysis, mass spectrometry, and computational chemistry. *Catal. Sci. Technol.* **7**, 4302–4314 (2017).
45. Flytzani-Stephanopoulos, M. Supported metal catalysts at the single-atom limit — a viewpoint. *Chin. J. Catal.* **38**, 1432–1442 (2017).
46. Kim, J., Kim, H.-E. & Lee, H. Single-atom catalysts of precious metals for electrochemical reactions. *ChemSusChem* **11**, 104–113 (2018).
47. Zhu, C., Fu, S., Shi, Q., Du, D. & Lin, Y. Single-atom electrocatalysts. *Angew. Chem. Int. Ed.* **56**, 13944–13960 (2017).
48. Qiao, B. T. et al. Ultrastable single-atom gold catalysts with strong covalent metal–support interaction (CMSI). *Nano Res.* **8**, 2913–2924 (2015).
49. Lin, J. et al. Remarkable performance of Ir_1/FeO_x single-atom catalyst in water gas shift reaction. *J. Am. Chem. Soc.* **135**, 15314–15317 (2013).
50. Lin, J. et al. Little do more: a highly effective Pt_1/FeO_x single-atom catalyst for the reduction of NO by H_2. *Chem. Commun.* **51**, 7911–7914 (2015).
51. Liang, J.-X. et al. Theoretical and experimental investigations on single-atom catalysis: Ir_1/FeO_x for CO oxidation. *J. Phys. Chem. C* **118**, 21945–21951 (2014).
52. Novotný, Z. et al. Ordered array of single adatoms with remarkable thermal stability: Au/Fe_3O_4(001). *Phys. Rev. Lett.* **108**, 216103 (2012).
53. Parkinson, G. S. et al. Carbon monoxide-induced adatom sintering in a Pd–Fe_3O_4 model catalyst. *Nat. Mater.* **12**, 724–728 (2013).
54. Bliem, R. et al. Cluster nucleation and growth from a highly supersaturated adatom phase: silver on magnetite. *ACS Nano* **8**, 7531–7537 (2014).
55. Bliem, R. et al. Adsorption and incorporation of transition metals at the magnetite Fe_3O_4(001) surface. *Phys. Rev. B* **92**, 075440 (2015).
56. Bliem, R. et al. Subsurface cation vacancy stabilization of the magnetite (001) surface. *Science* **346**, 1215–1218 (2014).
57. Zhang, S. et al. Catalysis on singly dispersed bimetallic sites. *Nat. Commun.* **6**, 7938 (2015).
58. Ma, X.-L., Liu, J.-C., Xiao, H. & Li, J. Surface single-cluster catalyst for N_2-to-NH_3 thermal conversion. *J. Am. Chem. Soc.* **140**, 46–49 (2018).
59. Bruix, A. et al. Maximum noble-metal efficiency in catalytic materials: atomically dispersed surface platinum. *Angew. Chem. Int. Ed.* **53**, 10525–10530 (2014).
60. Neitzel, A. et al. Atomically dispersed Pd, Ni, and Pt species in ceria-based catalysts: principal differences in stability and reactivity. *J. Phys. Chem. C* **120**, 9852–9862 (2016).
61. Dvorák, F. et al. Creating single-atom Pt–ceria catalysts by surface step decoration. *Nat. Commun.* **7**, 10801 (2016).
62. Zhang, S. et al. Solid frustrated-Lewis-pair catalysts constructed by regulations on surface defects of porous nanorods of CeO_2. *Nat. Commun.* **8**, 15266 (2017).
63. Zhang, B. et al. Stabilizing a platinum$_1$ single-atom catalyst on supported phosphomolybdic acid without compromising hydrogenation activity. *Angew. Chem. Int. Ed.* **55**, 8319–8323 (2016).
64. Huang, W. et al. Low-temperature transformation of methane to methanol on Pd_1O_4 single sites anchored on the internal surface of microporous silicate. *Angew. Chem. Int. Ed.* **55**, 13441–13445 (2016).
65. Cotton, A. G. W. F., Murillo, C. A. & Bochmann, M. *Advanced Inorganic Chemistry* 6th edn (Wiley, New York, 1999).
66. Peterson, E. J. et al. Low-temperature carbon monoxide oxidation catalysed by regenerable atomically dispersed palladium on alumina. *Nat. Commun.* **5**, 4885 (2014).
67. Kwak, J. H. et al. Coordinatively unsaturated Al^{3+} centers as binding sites for active catalyst phases of platinum on γ-Al_2O_3. *Science* **325**, 1670–1673 (2009).
68. Bulushev, D. A. et al. Single atoms of Pt-group metals stabilized by N-doped carbon nanofibers for efficient hydrogen production from formic acid. *ACS Catal.* **6**, 3442–3451 (2016).
69. Vilé, G. et al. A stable single-site palladium catalyst for hydrogenations. *Angew. Chem. Int. Ed.* **54**, 11265–11269 (2015).
70. Li, X. et al. Single-atom Pt as co-catalyst for enhanced photocatalytic H_2 evolution. *Adv. Mater.* **28**, 2427–2431 (2016).
71. Gao, G., Jiao, Y., Waclawik, E. R. & Du, A. J. Single atom (Pd/Pt) supported on graphitic carbon nitride as an efficient photocatalyst for visible-light reduction of carbon dioxide. *J. Am. Chem. Soc.* **138**, 6292–6297 (2016).
72. Li, F. Y., Li, Y. F., Zeng, X. C. & Chen, Z. F. Exploration of high-performance single-atom catalysts on support M_1/FeO_x for CO oxidation via computational study. *ACS Catal.* **5**, 544–552 (2015).
73. Choi, C. H. et al. Tuning selectivity of electrochemical reactions by atomically dispersed platinum catalyst. *Nat. Commun.* **7**, 10922 (2016).
74. Choi, M., Wu, Z. & Iglesia, E. Mercaptosilane-assisted synthesis of metal clusters within zeolites and catalytic consequences of encapsulation. *J. Am. Chem. Soc.* **132**, 9129–9137 (2010).
75. Fei, H. et al. Atomic cobalt on nitrogen-doped graphene for hydrogen generation. *Nat. Commun.* **6**, 8668 (2015).
76. Wu, H. et al. Highly doped and exposed Cu(i)–N active sites within graphene towards efficient oxygen reduction for zinc–air batteries. *Energy Environ. Sci.* **9**, 3736–3745 (2016).
77. Qiu, H.-J. et al. Nanoporous graphene with single-atom nickel dopants: an efficient and stable catalyst for electrochemical hydrogen production. *Angew. Chem. Int. Ed.* **54**, 14031–14035 (2015).
78. Cui, X. et al. A graphene composite material with single cobalt active sites: a highly efficient counter electrode for dye-sensitized solar cells. *Angew. Chem. Int. Ed.* **55**, 6708–6712 (2016).
79. Chen, Y. et al. Isolated single iron atoms anchored on N-doped porous carbon as an efficient electrocatalyst for the oxygen reduction reaction. *Angew. Chem. Int. Ed.* **56**, 6937–6941 (2017).
80. Chen, P. et al. Atomically dispersed iron–nitrogen species as electrocatalysts for bifunctional oxygen evolution and reduction reactions. *Angew. Chem. Int. Ed.* **56**, 610–614 (2017).
81. Zitolo, A. et al. Identification of catalytic sites for oxygen reduction in iron- and nitrogen-doped graphene materials. *Nat. Mater.* **14**, 937–942 (2015).
82. Zitolo, A. et al. Identification of catalytic sites in cobalt-nitrogen-carbon materials for the oxygen reduction reaction. *Nat. Commun.* **8**, 957 (2017).
83. Zhang, L. et al. Co–N–C catalyst for C–C coupling reactions: on the catalytic performance and active sites. *ACS Catal.* **5**, 6563–6572 (2015).
84. Liu, W. et al. Discriminating catalytically active FeN*x* species of atomically dispersed Fe–N–C catalyst for selective oxidation of C–H bond. *J. Am. Chem. Soc.* **139**, 10790–10798 (2017).
85. Yang, M. et al. Catalytically active Au-O(OH)*x* species stabilized by alkali ions on zeolites and mesoporous oxides. *Science* **346**, 1498–1501 (2014).
86. Yang, M. et al. A common single-site Pt(ii)–O(OH)*x*– species stabilized by sodium on "active" and "inert" supports catalyzes the water–gas shift reaction. *J. Am. Chem. Soc.* **137**, 3470–3473 (2015).
87. Wei, H. et al. Remarkable effect of alkalis on the chemoselective hydrogenation of functionalized nitroarenes over high-loading Pt/FeO_x catalysts. *Chem. Sci.* **8**, 5126–5131 (2017).
88. Zhang, L. et al. Efficient and durable Au alloyed Pd single-atom catalyst for the Ullmann reaction of aryl chlorides in water. *ACS Catal.* **4**, 1546–1553 (2014).
89. Lucci, F. R. et al. Controlling hydrogen activation, spillover, and desorption with Pd–Au single-atom alloys. *J. Phys. Chem. Lett.* **7**, 480–485 (2016).
90. Pei, G. X. et al. Ag alloyed Pd single-atom catalysts for efficient selective hydrogenation of acetylene to ethylene in excess ethylene. *ACS Catal.* **5**, 3717–3725 (2015).
91. Pei, G. X. et al. Performance of Cu-alloyed Pd single-atom catalyst for semihydrogenation of acetylene under simulated front-end conditions. *ACS Catal.* **7**, 1491–1500 (2017).
92. Feng, Q. et al. Isolated single-atom Pd sites in intermetallic nanostructures: high catalytic selectivity for semihydrogenation of alkynes. *J. Am. Chem. Soc.* **139**, 7294–7301 (2017).
93. Lucci, F. R. et al. Selective hydrogenation of 1,3-butadiene on platinum–copper alloys at the single-atom limit. *Nat. Commun.* **6**, 8550 (2015).
94. Liu, J. et al. Tackling CO poisoning with single-atom alloy catalysts. *J. Am. Chem. Soc.* **138**, 6396–6399 (2016).
95. Yang, M., Allard, L. F. & Flytzani-Stephanopoulos, M. Atomically dispersed Au–(OH)*x* species bound on titania catalyze the low-temperature water-gas shift reaction. *J. Am. Chem. Soc.* **135**, 3768–3771 (2013).
96. Wang, C., Yang, M. & Flytzani-Stephanopoulos, M. Single gold atoms stabilized on nanoscale metal oxide supports are catalytic active centers for various reactions. *AIChE J.* **62**, 429–439 (2016).
97. Guan, H. et al. Enhanced performance of Rh_1/TiO_2 catalyst without methanation in water–gas shift reaction. *AIChE J.* **63**, 2081–2088 (2017).
98. Ding, K. et al. Identification of active sites in CO oxidation and water–gas shift over supported Pt catalysts. *Science* **350**, 189–192 (2015).
99. Guo, L.-W. et al. Contributions of distinct gold species to catalytic reactivity for carbon monoxide oxidation. *Nat. Commun.* **7**, 13481 (2016).
100. Guan, H. et al. Catalytically active Rh sub-nanoclusters on TiO_2 for CO oxidation at cryogenic temperatures. *Angew. Chem. Int. Ed.* **55**, 2820–2824 (2016).
101. Therrien, A. J. et al. An atomic-scale view of single-site Pt catalysis for low-temperature CO oxidation. *Nat. Catal.* **1**, 192–198 (2018).

102. Wang, C. et al. Water-mediated Mars–Van Krevelen mechanism for CO oxidation on ceria-supported single-atom Pt_1 catalyst. *ACS Catal.* **7**, 887–891 (2017).
103. Li, L. et al. Origin of the high activity of Au/FeO_x for low-temperature CO oxidation: direct evidence for a redox mechanism. *J. Catal.* **299**, 90–100 (2013).
104. Nie, L. et al. Activation of surface lattice oxygen in single-atom Pt/CeO_2 for low-temperature CO oxidation. *Science* **358**, 1419–1423 (2017).
105. Yi, N., Si, R., Saltsburg, H. & Flytzani-Stephanopoulos, M. Active gold species on cerium oxide nanoshapes for methanol steam reforming and the water gas shift reactions. *Energy Environ. Sci.* **3**, 831–837 (2010).
106. Gu, X.-K. et al. Supported single Pt_1/Au_1 atoms for methanol steam reforming. *ACS Catal.* **4**, 3886–3890 (2014).
107. Lin, L. et al. Low-temperature hydrogen production from water and methanol using Pt/α-MoC catalysts. *Nature* **544**, 80–83 (2017).
108. Bayatsarmadi, B., Zheng, Y., Vasileff, A. & Qiao, S.-Z. Recent advances in atomic metal doping of carbon-based nanomaterials for energy conversion. *Small* **13**, 1700191 (2017).
109. Wu, G. & Zelenay, P. Nanostructured nonprecious metal catalysts for oxygen reduction reaction. *Acc. Chem. Res.* **46**, 1878–1889 (2013).
110. Cheng, N. et al. Platinum single-atom and cluster catalysis of the hydrogen evolution reaction. *Nat. Commun.* **7**, 13638 (2016).
111. Liu, J. et al. High performance platinum single atom electrocatalyst for oxygen reduction reaction. *Nat. Commun.* **8**, 15938 (2017).
112. Deng, J. et al. Triggering the electrocatalytic hydrogen evolution activity of the inert two-dimensional MoS_2 surface *via* single-atom metal doping. *Energy Environ. Sci.* **8**, 1594–1601 (2015).
113. Zhang, S. et al. High catalytic activity and chemoselectivity of sub-nanometric Pd clusters on porous nanorods of CeO_2 for hydrogenation of nitroarenes. *J. Am. Chem. Soc.* **138**, 2629–2637 (2016).
114. Porosoff, M. D., Yan, B. & Chen, J. G. Catalytic reduction of CO_2 by H_2 for synthesis of CO, methanol and hydrocarbons: challenges and opportunities. *Energy Environ. Sci.* **9**, 62–73 (2016).
115. Kwak, J. H., Kovarik, L. & Szanyi, J. Heterogeneous catalysis on atomically dispersed supported metals: CO_2 reduction on multifunctional Pd catalysts. *ACS Catal.* **3**, 2094–2100 (2013).
116. Kwak, J. H., Kovarik, L. & Szanyi, J. CO_2 reduction on supported Ru/Al_2O_3 catalysts: cluster size dependence of product selectivity. *ACS Catal.* **3**, 2449–2455 (2013).
117. Li, S. et al. Tuning the selectivity of catalytic carbon dioxide hydrogenation over iridium/cerium oxide catalysts with a strong metal–support interaction. *Angew. Chem. Int. Ed.* **56**, 10761–10765 (2017).
118. Cheng, M.-J., Clark, E. L., Pham, H. H., Bell, A. T. & Head-Gordon, M. Quantum mechanical screening of single-atom bimetallic alloys for the selective reduction of CO_2 to C_1 hydrocarbons. *ACS Catal.* **6**, 7769–7777 (2016).
119. Back, S., Lim, J., Kim, N.-Y., Kim, Y.-H. & Jung, Y. Single-atom catalysts for CO_2 electroreduction with significant activity and selectivity improvements. *Chem. Sci.* **8**, 1090–1096 (2017).
120. Back, S. & Jung, Y. TiC- and TiN-supported single-atom catalysts for dramatic improvements in CO_2 electrochemical reduction to CH_4. *ACS Energy Lett.* **2**, 969–975 (2017).
121. Sarfraz, S., Garcia-Esparza, A. T., Jedidi, A., Cavallo, L. & Takanabe, K. Cu–Sn bimetallic catalyst for selective aqueous electroreduction of CO_2 to CO. *ACS Catal.* **6**, 2842–2851 (2016).
122. Zhao, C. et al. Ionic exchange of metal–organic frameworks to access single nickel sites for efficient electroreduction of CO_2. *J. Am. Chem. Soc.* **139**, 8078–8081 (2017).
123. Yang, H. B. et al. Atomically dispersed Ni(I) as the active site for electrochemical CO_2 reduction. *Nat. Energy* **3**, 140–147 (2018).
124. Genovese, C. et al. Operando spectroscopy study of the carbon dioxide electro-reduction by iron species on nitrogen-doped carbon. *Nat. Commun.* **9**, 935 (2018).
125. Yamanaka, I., Onizawa, T., Takenaka, S. & Otsuka, K. Direct and continuous production of hydrogen peroxide with 93% selectivity using a fuel-cell system. *Angew. Chem. Int. Ed.* **42**, 3653–3655 (2003).
126. Siahrostami, S. et al. Enabling direct H_2O_2 production through rational electrocatalyst design. *Nat. Mater.* **12**, 1137–1143 (2013).
127. Verdaguer-Casadevall, A. et al. Trends in the electrochemical synthesis of H_2O_2: enhancing activity and selectivity by electrocatalytic site engineering. *Nano Lett.* **14**, 1603–1608 (2014).
128. Liu, G. et al. MoS_2 monolayer catalyst doped with isolated Co atoms for the hydrodeoxygenation reaction. *Nat. Chem.* **9**, 810–816 (2017).
129. Wang, Y.-G., Yoon, Y., Glezakou, V.-A., Li, J. & Rousseau, R. The role of reducible oxide–metal cluster charge transfer in catalytic processes: new insights on the catalytic mechanism of CO oxidation on Au/TiO_2 from ab initio molecular dynamics. *J. Am. Chem. Soc.* **135**, 10673–10683 (2013).
130. Wang, Y.-G., Mei, D. H., Glezakou, V. A., Li, J. & Rousseau, R. Dynamic formation of single-atom catalytic active sites on ceria-supported gold nanoparticles. *Nat. Commun.* **6**, 6511 (2015).
131. Liu, J.-C., Wang, Y.-G. & Li, J. Toward rational design of oxide-supported single-atom catalysts: atomic dispersion of gold on ceria. *J. Am. Chem. Soc.* **139**, 6190–6199 (2017).
132. Wang, J. et al. Formation, migration, and reactivity of Au–CO complexes on gold surfaces. *J. Am. Chem. Soc.* **138**, 1518–1526 (2016).
133. Eren, B. et al. Activation of Cu(111) surface by decomposition into nanoclusters driven by CO adsorption. *Science* **351**, 475–478 (2016).
134. Bliem, R. et al. Dual role of CO in the stability of subnano Pt clusters at the Fe_3O_4(001) surface. *Proc. Natl Acad. Sci. USA* **113**, 8921–8926 (2016).
135. Horch, S. et al. Enhancement of surface self-diffusion of platinum atoms by adsorbed hydrogen. *Nature* **398**, 134–136 (1999).
136. Matsubu, J. C. et al. Adsorbate-mediated strong metal–support interactions in oxide-supported Rh catalysts. *Nat. Chem.* **9**, 120–127 (2017).
137. Li, C. et al. Single atom dispersed Rh-biphephos&PPh_3@porous organic copolymers: highly efficient catalysts for continuous fixed-bed hydroformylation of propene. *Green Chem.* **18**, 2995–3005 (2016).
138. Lang, R. et al. Hydroformylation of olefins by a rhodium single-atom catalyst with activity comparable to $RhCl(PPh_3)_3$. *Angew. Chem. Int. Ed.* **55**, 16054–16058 (2016).
139. Wang, L. et al. Atomic-level insights in optimizing reaction paths for hydroformylation reaction over Rh/CoO single-atom catalyst. *Nat. Commun.* **7**, 14036 (2016).
140. Sahu, S. & Goldberg, D. P. Activation of dioxygen by iron and manganese complexes: a heme and nonheme perspective. *J. Am. Chem. Soc.* **138**, 11410–11428 (2016).
141. He, L., Weniger, F., Neumann, H. & Beller, M. Synthesis, characterization, and application of metal nanoparticles supported on nitrogen-doped carbon: catalysis beyond electrochemistry. *Angew. Chem. Int. Ed.* **55**, 12582–12594 (2016).
142. DeRita, L. et al. Catalyst architecture for stable single atom dispersion enables site-specific spectroscopic and reactivity measurements of CO adsorbed to Pt atoms, oxidized Pt clusters, and metallic Pt clusters on TiO_2. *J. Am. Chem. Soc.* **139**, 14150–14165 (2017).
143. Liu, J. C. et al. Heterogeneous Fe_3 single-cluster catalyst for ammonia synthesis via an associative mechanism. *Nat. Commun.* **9**, 1610 (2018).
144. Yan, H. et al. Bottom-up precise synthesis of stable platinum dimers on graphene. *Nat. Commun.* **8**, 1070 (2017).
145. Ji, S. et al. Confined pyrolysis within metal–organic frameworks to form uniform Ru_3 clusters for efficient oxidation of alcohols. *J. Am. Chem. Soc.* **139**, 9795–9798 (2017).
146. Shan, J., Li, M., Allard, L. F., Lee, S. & Flytzani-Stephanopoulos, M. Mild oxidation of methane to methanol or acetic acid on supported isolated rhodium catalysts. *Nature* **551**, 605–608 (2017).
147. Tang, Y. et al. Single rhodium atoms anchored in micropores for efficient transformation of methane under mild conditions. *Nat. Commun.* **9**, 1231 (2018).
148. Jasion, V. S. & Poulos, T. L. *Leishmania major* peroxidase is a cytochrome *c* peroxidase. *Biochemistry* **51**, 2453–2460 (2012).

Acknowledgements
The authors thank J. Liu, B. Qiao, Y.-G. Wang, X.-F. Yang and R. Rousseau for fruitful discussions. This work is supported by the National Key Projects for Fundamental Research and Development of China (2016YFA0202801), National Natural Science Foundation of China (21690080, 21690084, 21721004, 21673228, 21522608, 21503219, 21672210, 21590792 and 91645203), and the Strategic Priority Research Program of the Chinese Academy of Sciences (XDB17000000 and 17020100). The authors thank Y. Ren, S. Niu, W. Liu, M. Zhou, J.-C. Liu and X. Yang for assisting in the preparation of some of the figures.

Author contributions
All authors contributed equally to the preparation of this manuscript.

Competing interests
The authors declare no competing interests.

Publisher's note
Springer Nature remains neutral with regard to jurisdictional claims in published maps and institutional affiliations.